The water balance equation of paddy rice is : Q=P+I-E-R-G, Q is diurnal variability of water, P is precipitation, I is irrigation, E is evapotranspiration, R is run-off, G is seepage loss. With the plastic film-bottom sandy paddy, both R and G are 0. After simplication, The equation is Q= P+I-E. According to the equation, two kinds of water budget were measured. Table 2 shows the diurnal variability of water use on sandy paddy using micro-meteorology, Figure 2 reports the dynamics of eva-poration and transpiration during growth in sandy paddy using field water balance methods.

The diurnal maximum of evapotranspiration at 14-15pm, the maximum of condensation is at 04-05am, Q=-2.045 kg/m2.The dynamics of E is less regular because of cloudy weather.

Water consumption shows in Figure 2 (EE: evaporation, ET: transpiration), it indicates ET= EE in the rice tillering later, early ET<EE, later ET>EE. The maximum of EE is in middle tillering, at this time, the plants are small and large bare areas exist. EE is the major factor in water con-sumption. With plant growth, the bare soil-area decrease, ET than become the major water consu-mption. The maximum of ET is between boot stage and heading stage. After the milk stage, ET be-come small. The total water consumption during growth in 4 months was measured in all period, deep water irrigation is1489.3mm, shallow and wet irrigation is1195.2mm.EE share 30 %, ET share 70% of total water consumption.
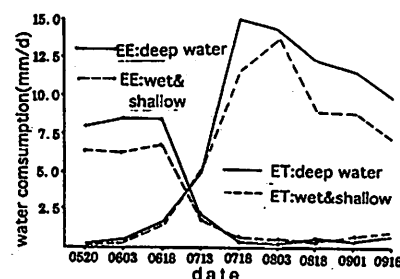

Figure 2.Dynamics of Water Consumption

4.3 Sandy paddy ecosystem

4.3.1 Soil temperature

Soil temperature is a heat index reflecting the energy transfer in eco-system. The difference of soil tempe-ratures between sandy paddy and sand dune are very large (Figure 3). The profiles on sandy paddy are approxi-mately vertical line, it shows that the exchange of heat up and down is very little. The sand paddy ecosystem is re-latively state compared to sand dune.
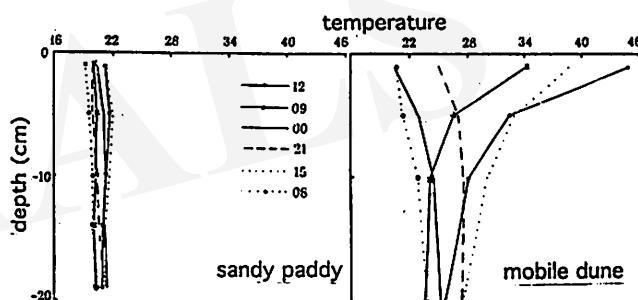

Figure 3. Soil Temperature Profile in Sandy Paddy and Sand Dune

4.3.2 Dynamics of nutrient and soil organic matter

With fertilization and abundant rice residues, the nutrient and soil organic matter(SOM) increase in sandy paddy compared to the sand dune. Soil increased after planting of rice.Total nitrogen increa-ed from 0.06 (dune) to 0.14 g/kg(paddy), total Phosphorus from 0.1 to 0.24 g/kg, but total pota-tassium were appropriately the small.

Table 3. Dynamic of Nutrient on Sandy Paddy (g/kg)

Total Nutrient			Quick Results Nutrient(%)		
N	P2O5	K2O	N	P2O5	K2O
Sand Dune 0.06	0.010	2.75	1.24	1.38	2.75
Sandy #CF 0.14	0.24	2.8	1.63	2.45	3.80
Paddy CM 0.28	0.37	2.8	2.00	5.16	9.50
M 0.22	0.26	2.8	2.79	3.78	10.05

#CF: chemical fertilizer plot,CM: chemical+manure plot, M: manure plot

Table 4.Dynamics of Organic Matter on Sandy Paddy

Items	Sand Dune		Sandy Paddy	
		1st year	2nd year	3rd year
OM (%)	0.42	0.53	1.03	0.90
Residues(kg/ha)	1109.54		3591.36	
Remaining Amount	432.2		689.86	
Decomposition After One Year(kg/ha)				

SOM on paddy is a major nutrient source for rice and, is the basic for the formation of humus colloids (Cao,1993). Sandy soils have low organic matter because of wind and water erosion. Ecotechniques of water-saving rice cultivation on sandy land increase the plant produtivity and rice residues. The paddy environment prevents organic matter loss. After cultivation rice for one year, SOM increase. The residues of rice roots and stubble in sandy paddy were 3591.36 kg/ha, approximately half of the residues decompose in next growth stage (Zhao,1994). Because of increased SOM, the chemical and physical characteristics of the soil are improved and the soil productivity of sandy land is raised.

4.4 Input and output on sandy paddy

The economic benifits determine whether an agricultural system is successful. During the first year of sandy paddy, production is 9,060 Chinese Yuan (CY). The return is low, because of the high costs of irrigation and plastic film. After one year, the ratio of output/input is 3.1. The purity benifits rise to 14,865 CY/ha/yr(table5). The plastic film in paddy does not decompose and can be used many years. In addition, New arable land is increasd and desertification is decreased.

Table 5. Cost of Input and Output on Three Farm Land (CY/ha/ per year)

Items	Sandy Paddy		Tranditional Paddy	Corn Land
	1st yr	After 1yr		
Input(total)	30,375	7,185	8,940	6,510
plastic film	4,200	0	0	0
irrigation	18,000	4,500	450	300
fertilizer	3,990	3,600	3,180	3,120
water cost	1,110	1,110	1,335	240
seedling	900	900	1,050	480
land cost	0	0	750	900
labour	2,175	1,125	1,725	1,470
Output(total)	21,315	22,050	18,559	14,412
grain	19,575	20,250	17,044	12,657
straw	1,740	1,800	1,515	1,755
Ratio:				
Input / Output	0.7	3.1	2.1	2.2

5.Conclution

Environmental degradation and poor economic conditions are a serious problem in sandy semiarid regions.The proposal strategies are optimal for natural resource utilization are to promoting the efficient utilization and reclamation of desert ecosystems. The ecotechniques for rice production are practical for the region.The approach helps control desertification and increase rice production , and have a high economic income. However, the premise of their application is based on abundant water availbility. They are labour intensive, require skill and capital. The farming system is suitable for a family.

Acknowledgements

Reference

Cao, J .M. (1993), Rice Farming in Jiling,Beijin, pp125-126
Cheng, D. ect. (1984), J. of Desert Research, Vol.6 (2) : 35-38
Huang, X. tc. (1995), J. of Desert Research, Vol.15,Supp.1:17-24
Liu, X.M.ect. (1995), J. of Desert Research, Vol.15, Supp.1:1-5
Liang, G. (1983), Rice Ecology,Beijin, pp229-263
Matsushima, (1987), New Techniques of Rice Cultivation, Jiling, pp85-90
Richmond, A. (1987), Desert Research of World, 2: 21-22
Wu, G. ect. (1981), The Theory and Technique of Rice Cultivation, pp316-320
Zhao, X. etc. (1995), J. of Desert Research, Vol. 15, Supp.1: 49-52

Yield Improvement of vegetables by using a super-water-absorbent polymer in sandy soil

Toshihiro YAMAZAKI[*], Masanao Matsumoto[*], Jiro ASANO[**] and Hideshige TODA[*]

Abstract-Effect of addition of a super-water-absorbent polymer (starch-acrylate graft copolymer) on vegetable yield was studied in sandy soil. Addition of the polymer to sandy soil (10-30 kg/are) increased yields of tomato (290-380%, control= 100%), pak choi (170-220%), turnip (130-200%), cabbage (105-140%), and daikon (140%). This improvement in vegetable yield was due to the increase in retention efficiency in both water and nutrients. No residual effect was observed in the next cultivation for the several types of polymers examined.

Key Words: super-water-absorbent polymer, vegetable yield, sandy soil

1. Introduction

The validity of super-water-absorbent polymers in agricultural use has been shown in raising of seedling, greening, reducing watering, and growth of some vegetables (Takeuchi et al., 1983; Toyama, 1986; Ouchi et al., 1989). However the plant species studied are still restricted. In the present study, the validity of a super-water-absorbent polymer for the improvement of yield was examined in several vegetable species in sandy soil, in which water and nutrients retentivity is generally low.

2. Materials and Methods

2.1 Cultivation experiments
The starch-acrylate graft copolymer (SANWET IM-300, Sanyo Kasei) was added to sandy soil (Sand-dune Regosol) in the weight ratios of 0, 1, 2, and 3g/kg air-dry sand (corresponding to 0, 10, 20, and 30 kg/are,1are=100m^2) in the small pot experiments, or 0, 10, 20, and 30 kg/are in the large pot and field experiments. Tomato was cultivated in a small pot (1/2000are=0.05m^2), pak choi and daikon in a large bottomless pot (0.4m^2) embedded in the field, and turnip and cabbage in the field. The residual effect of polymers of several types were examined by the cucumber-melon cultivation in a greenhouse, and by the

* Coastal Sand Branch, Shizuoka Agr. Exp. Sta., Kaigan 4433, Godo, Hamaoka, Shizuoka 437-16, Japan (Fax: +81-537-86-5244)
** Morioka Branch, Natl. Inst. Vegetable, Ornamental Crops & Tea, Iwate 020-01, Japan

komatsuna-pak choi cultivation under outdoor conditions. Water was supplied over all treatments when wilting was observed in the control. Cultivation and manuring practices were standard in Shizuoka (Shizuoka-ken, 1981). Most cultivation experiments were done in duplicate.

2.2 pF-soil moisture curve The pF-soil moisture curve was made for the sandy soil added with the copolymer (0, 1, 2, and 3g/kg) by using sand column method and centrifuging method.

2.3 Leaching experiment The sandy soil added with the copolymer (0, 1, 2, and 3g/kg) and fertilizer (40mg N, P_2O_5, K_2O/kg, 60mg CaO/kg, 30mg MgO/kg) was packed into glass jars (7.6cm diameter, 12cm height, equipped with bottom mouth). About 200ml of distilled water was dripped, and the initial effluent of 100ml was analyzed for nutrients.

3. Results and Discussions

Addition of the copolymer to the sandy soil (10-30 kg/are) increased yields of tomato (290-380%, control= 100%), pak choi (170-220%), turnip (130-200%), cabbage (105-140%), and daikon (140%) (Fig. 1). There is a significant relationship between the amount of the copolymer added and the vegetable yields (P<0.1). The yield improvement was more remarkable in spring-summer crops (pak choi and turnip) than in fall-winter crops (cabbage and daikon). In the cultivation of tomato, blossom end rot
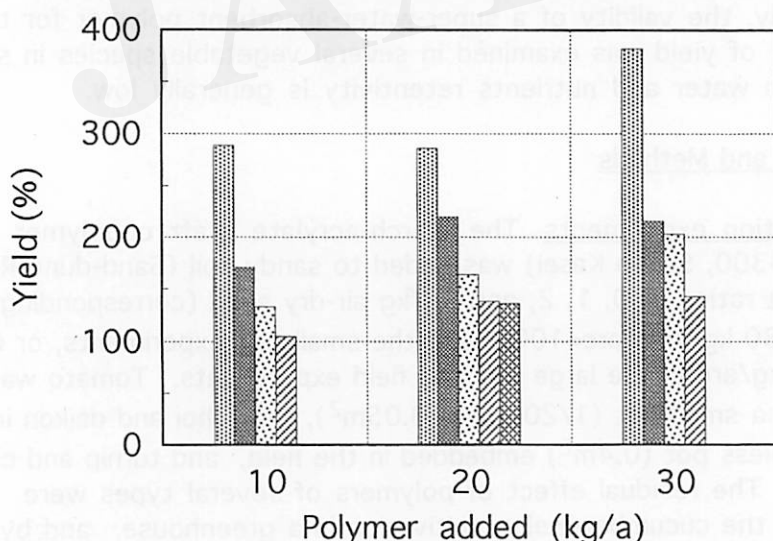

Fig. 1 Effect of polymer addition on vegetable yield.
▦ tomato   ▧ turnip   ▨ daikon
▩ pak choi   ▨ cabbage

(calcium shortage) spread and inhibited the thickening the fruit growth in the control (no polymer addition). The calcium shortage is considered to be accelerated by radical change in soil moisture. In this case the addition of the copolymer might alleviate the moisture conditions in soil, and indirectly improve the yield of tomato.

In the cultivation experiments in greenhouse and outdoor field using various types of super-water-absorbent polymers, yield improvement of the 1st cultivation (cucumber, 120-130%; komatsuna, 110-180%) was observed for all the polymers examined (Fig. 2). No residual effect of the polymers was observed in the next culture. The function of the polymers might be lost due to biodegradation, physical degradation in molecular structure, and/or adhesion of cations such as calcium and magnesium abundant in soil.
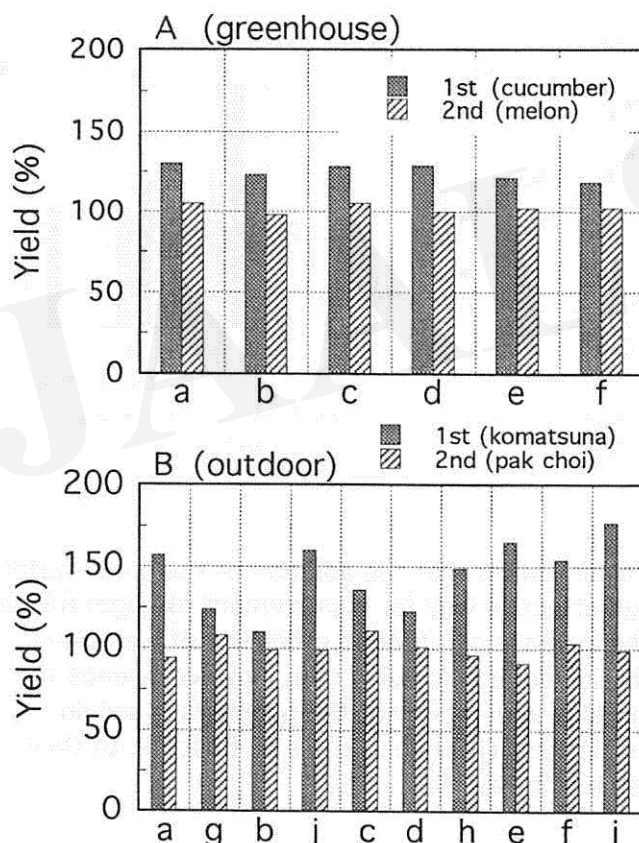
Fig. 2 Effect of polymer addition on vegetable yield of the1st and 2nd cultivations. The polymers (10kg/a) were added at the start of the 1st cultivation.
a,g: starch-acrylate type; b, j: CMC type; c, isobutylene type; d, h: acrylonitrile type; e, f, i: acrylate type

The addition of the copolymer to the sandy soil showed increase in the amount of water available for plant (pF=1.7-3.8 in sandy soil) (Fig. 3), and decrease in solid phase, increase in liquid phase and little change in gaseous phase. This result clearly shows that the addition of the copolymer increases the retention efficiency of water by sandy soil without losing air permeability. Excess addition of a super-water-absorbent polymer to the soil, however, may result in reduction in gaseous phase and causes adverse effect in vegetable growth (Takeuchi et al., 1983).

Leaching of NH_4-N, K_2O, CaO, and MgO from the sandy soil was reduced to 50-70% of the control by the addition of the copolymer(Fig. 4). This result shows that the polymer addition to the sandy soil increases retention efficiency in nutrients as well as water.
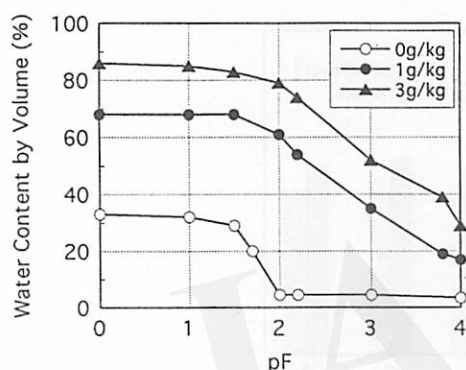

Fig. 3 Effect of polymer addition on moisture characteristics of sandy soil.
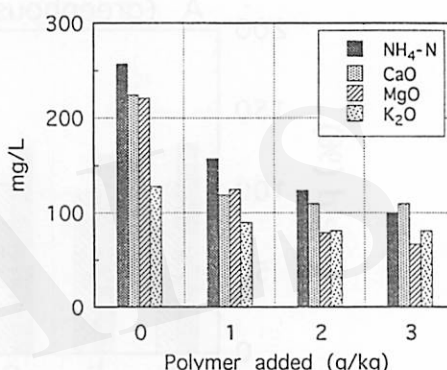
Fig. 4 Effect of polymer addition on nutrient leaching from sandy soil.

4. Conclusion

The present results clearly show that the addition of the super-water-absorbent polymer is an effective way for improvement of vegetable yields in sandy soil, due to the increase in retention efficiency of water and nutrients.   Each successive vegetable cultivation, however, needs the polymers addition. This lack in durability of the polymers in soil, in addition to their expensiveness (800 yen/kg), is an obstacle to their practical use in vegetable culture.

References
Ouchi, S., Nishikawa, A. and Kamada, E. (1990): Japanese Journal of Soil Science and Plant Nutrition , 61 : 606-613.
Shizuoka-ken (1981): "Shizuoka-ken Dojouhiryou Handbook" (Shizuoka Fertilizer Handbook, in Japanese), pp.444, Bunkadou, Shizuoka.
Takeuchi, Y. and others (1983): Sand Dune Research, 30 : 262-269.
Toyama, M. (1986): Agriculture and Horticulture , 61 : 1087-1092.

Water resources & management

W1: Chaired by E. Adar & Y. Hirosawa
W2: Chaired by M. Garduno & Y. Hiraga

Contents

Original Articles

A Brine Chemistry Model to Simulate the Formation of Evaporites in Waters Undergoing Desiccation

Kenneth K. TANJI*

Abstract - An opportunity exists to harvest salts from saline waters that are no longer usable through solar evapoconcentration. A brine equilibrium chemistry model (C-SALT) has been formulated to simulate the mineral precipitation of evaporites from desiccating hypersaline waters. C-SALT is a specific-ion interaction model based on the Pitzer equations. It has been validated with data from desiccating seawater and then utilized to simulate the sequence of evaporite formation when saline agricultural drainage waters are desiccated to near dryness, producing thenardite, halite, gypsum, etc.

Key Words: Pitzer equations, dissolved mineral salts, halite, thenardite, gypsum.

1. Introduction

Since water is a scarce resource in arid regions, water should be used until no longer usable. Saline waters may be used for purposes not requiring freshwaters, but such uses are limited. An opportunity exists to harvest salts from brines and other hypersaline waters to more fully utilize this often wasted resource. This paper describes C-SALT (Smith et al., 1995), an equilibrium chemistry model based on the Pitzer equations, to simulate evaporite formation when saline agricultural drainage waters are evapoconcentrated.

2. Theoretical Basis of Model

Geochemical equilibrium models have been formulated to compute chemical speciation and solubility of minerals in aqueous systems (Jenne, 1979). In these models the activity of solute species in heterogeneous solutions is obtained from the product of its ionic molar concentration and its ionic activity coefficient. Most of these models are based on the extended Debye-Huckel (eq. 1) or the Davies equation (eq. 2) to calculate the single-ion activity coefficients as a function of ionic strength for longer-range electrostatic forces, and use thermodynamic values for shorter-range ion-ion association as well as mineral solubility. The Debye-Huckel and the Davies equation, however, are only applicable to ionic strengths up to 0.5 molar which is less than seawater. Therefore, a number of investigators (Melchior and Bassett, 1990) have resorted to the use of the Pitzer equations (1979) which is applicable to ionic strengths up to about 20 molal (eq. 3).

---

*Dept. of Land, Air and Water Resources, Hydrologic Science Program, Univ. of California, Davis, California 95616 USA (Fax: +1-916-752-5262)

$$\log \gamma_i = \frac{-0.05085 z_i I^{0.5}}{1 + 0.3281 a I^{0.5}} \tag{1}$$

$$\log \gamma_i = -0.05085 z_i [\{I^{0.5} / (1 + I^{0.5})\} - 0.3I] \tag{2}$$

$$\ln \gamma_i = \ln \gamma_i^{DH} + \Sigma B_{ij}(I) m_j + \Sigma_j \Sigma_k C_{ijk} m_j m_k + \ldots \tag{3}$$

where γ is the ionic activity coefficient of solute species i, z is the charge of the ion, I is the ionic strength, a is the ion-size parameter, DH is Debye-Huckel, m is molality, $B_{ij}(I)$ is the second virial coefficient for ion pairs between species i and j that are dependent on ion concentrations and I, and C_{ijk} is the third virial coefficients for ion triplets between species i, j and k that are dependent on only ion concentrations and not I. The binary ion pairs may consist of cation-anion, cation-cation or anion-anion pairs, and the ternary ion triplets, cation-cation-anion, and anion-anion-cation ion associations. In addition, ion-neutral and ion-ion-neutral interactions are considered. Consequently, the Pitzer equations are known as the specific-ion interaction model. The Pitzer equations is based on Gibbs excess free energy of mixing comprised of the difference in change in free energy between a real mixture of solutes and ideal mixture. Computations involve minimization of the excess free energy of mixing.

3. C-SALT

C-SALT (Smith et al., 1995) requires input data on initial stoichiometric concentration of ions, thermodynamic file data on ion pairs, triplets and solid phase minerals, extent of evapoconcentration (a concentration factor of one will give equilibrium speciation) or dilution, and temperature corrections for stability constants over 10 to 40 °C. Carbonate chemistry and pH are handled specially. If pH is not specified, C-SALT will compute pH from constituents comprising total alkalinity. If the calculated I is less than 0.4 m, the Davies equation is used to calculate γ_i. Output data is extensive including speciation of free ions as well as binary and ternary associated ions, and moles/kg of precipitated evaporites.

4. Validation with Seawater

The single-ion activity coefficients in seawater calculated by C-SALT differed only slightly with those reported by Whitfield (1975). Simulation runs on the desiccation of seawater with and without carbonate species were in good agreement with those of Harvie et al. (1980, 1982). Table 1 gives the chemistry of standard seawater. It should be noted that seawater is supersaturated with dolomite [CaMg(CO3)2] but dolomite does not form in seawater because of kinetic limitations.

237

Table 1. Chemistry of Seawater and Peck Pond in moles/m^3.

Constituents	Seawater	Peck Pond
pH	7.90	7.39
Na	479.3	94.0
Mg	54.5	4.68
Ca	10.6	11.8
K	10.1	0.19
Cl	558.7	20.3
SO4	28.9	45.3
HCO3	2.93	16.3
CO3	0.008	0

Table 2 gives representative computed results for seawater desiccation without dolomite. Calcite [CaCO3] and magnesite [MgCO3], not shown, are present at all concentration factors (CF) while halite [NaCl] begins to form before a CF of 15 and thenardite [Na2SO4] before a CF of 50.

Table 2. Desiccation of seawater without dolomite.

Concentration Factor	1	10	20	50
Ionic strength (m)	0.630	6.537	7.927	10.21
Density (g/cm3)	1.028	1.249	1.312	1.472
Osmotic coefficient	0.905	1.181	1.195	1.103
Activity of water	0.982	0.773	0.742	0.732
Calcite (mol/kg)	5.60E-3	1.18E-1	2.39E-1	6.15E-1
Halite,(mol/kg)	0	0	5.289	21.707
Thenardite,(mol/kg)	0	0	0	9.50E-2

5. Applications: Desiccation of Evaporation Ponds

Saline agricultural drainage waters impounded into evaporation ponds are dissipated by solar desiccation and produces salts. For illustrative purposes, Table 3 contains simulated evapoconcentration of drain waters impounded in Peck Pond. Unlike seawater which is dominated by Na and Cl ions, this drainwater is dominated by Na and SO4 ions (Table 1). Calcite is the first mineral to precipitate but by a CF of 15, it is depleted because of Ca competition for formation of gypsum and glauberite [Na2Ca(SO4)2]. Thenardite begins to form by a CF of 80 and halite at a CF of 90. All of these minerals were detected by X-ray diffraction analyses of salt crusts sampled from Peck Pond.

Based on numerous runs, Table 4 gives evaporites expected to form in the dessiccating ponds under increasing CFs and varying water compositions. At early stages of evapoconcentration, calcite

and gypsum are the most common evaporites formed, and at later stages, thenardite and halite.

Table 3 Simulated desiccation of waters in Peck Pond

Concentration factor	1	10	50	100
Ionic strength (m)	0.139	1.368	6.038	8.877
Activity of water	0.997	0.974	0.857	0.748
Calcite (mol/kg)	2.60E--3	1.99E-2	0	0
Gypsum (mol/kg)	0	8.20E-2	1.51E-1	0
Glauberite (mol/kg)	0	0	6.75E-2	4.62E-1
Thenardite (mol/kg)	0	0	0	4.09E-1
Halite (mol/kg)	0	0	0	8.33E-1

Table 4. Expected formation of common evaporites depending on water type and concentration factor

Water type	Most common minerals for CF ranges		
	0-30	30-60	60-100
Na, Cl = SO$_4$	Calcite	Calcite, Mirabilite	Thenardite
Na, Cl < SO$_4$	Calcite, Gypsum	Gypsum	Glauberite, Thenardite
Na, Cl > SO$_4$	Calcite, Gypsum	Thenardite, Halite	Halite, Glauberite

6. Conclusions

C-SALT is a flexible equilibrium brine chemistry model capable of handling ionic strengths up to 20 molal. It has been validated with seawater chemistry and its desiccation sequence. And it has been successfully applied to the desiccation of saline agricultural drainage waters and identification of various mineral species as a function of evapoconcentration factors.

7. References

Harvie, C., Weare, J.H., Hardie, L.A. and Eugster, H.P. (1980): Science 208:498-500

Harvie, C., Eugster, H.P., and Weare, J.H. (1982): Geochim. Cosmochim. Acta 46:1603-1618.

Jenne, E.A., editor. (1979). Chemical Modeling in Aqueous Systems. Amer. Chemical Society.

Melchior, D.C., and Bassett, R.L., editors. (1990): Chemical Modeling of Aqueous Systems II. Amer. Chemical Society.

Pitzer, K.S. (1979): Activity Coefficients in Electrolyte Solutions, R.M. Pytkowic, editor, CRC Press.

Smith, G.R., Tanji, K.K., Jurinak, J.J. and Burau, R.G. (1995): Chemical Equilibrium and Reaction Models, Soil Science Society of America Special Publication 42.

Whitfield, M. (1979): Activity Coefficients in Electrolyte Solutions, R.M. Pytkowic, editor, CRC Press.

Simplified Model for Simulation of Artificial Rainfall and Water Circulation.

Satoshi MATSUDA*, Toshiyuki GOTO* and Yasunori OKANO*

Abstract · Efficient water supply and control is essential in greening of arid and semiarid land for CO_2 fixation on an enormous scale. Fresh water must be obtained efficiently from salt water using abundantly available solar heat. A possible alternative may be artificial rainfall. In this study, a simplified model for simulation of artificial rainfall and water circulation is proposed to examine the possibility of this means of water supply. The basic conditions required for rainfall are humid air and ascending current. We constructed a simplified mathematical model in which essential factors such as heat balance, evaporation rate, and ascending current are integrated.

Key Words : Artificial Rainfall, Simulation, Heat Balance, Evaporation, Ascending Current

1. Introduction

To deal with the global warming issue, various measures of CO_2 recovery and disposal have been proposed and tried. In these measures of CO_2 fixation, greening of arid and semiarid land is though to be one of the most hopeful alternatives, because the surface biosphere has a large potential to fix carbon and greening itself is ecologically sound and variable alternative. The statement above, however, does not mean that the greening is an easy countermeasure against the global warming issue. First, it is estimated that land area of about 10^4 km^2(=100 km × 100 km) is necessary to fix 10^8t·C if the density of plant biomass is the same level as in temperate forest. Second, a huge amount of artificial energy input may be required for water supply and control, which is essential in the management of arid and semiarid land. Fresh water must be obtained efficiently from salt water using abundantly available solar heat. A possible alternative may be artificial rainfall. The basic conditions required for rainfall are humid air and ascending current. The former may be obtained if large scale artificial shallows can be constructed to accelerate the evaporation of sea water, and the latter can be generated by controlling the temperature of the ground surface on a large scale. In the first step of research, it is necessary to examine quantitatively the possibility of this concept using model simulation before on site experiment on a real scale. Thus, we tried in this study to construct a simplified mathematical model for simulation of artificial rainfall and water circulation, in which essential factors such as heat balance, evaporation rate, and ascending current are integrated.

2. Heat Balance and Evaporation Rate

Suppose that there is a shallow water layer on the ground surface. When solar energy is the sole input, and outputs are the fluxes of sensible and latent heat, and the flux by heat conduction to underground as shown in Fig. 1. The energy balance of this layer at steady state can be expressed as

$$Rn = H + lE + G \tag{1}$$

where net radiation absorbed by the ground surface Rn is given as

$$Rn = R\downarrow - \sigma Ts^4 \tag{2}$$

The term $R\downarrow$ is defined as

$$R\downarrow = (1-ref) S\downarrow + L\downarrow \tag{3}$$

where

$$S\downarrow = So\downarrow (1-ref') \tag{4}$$

and

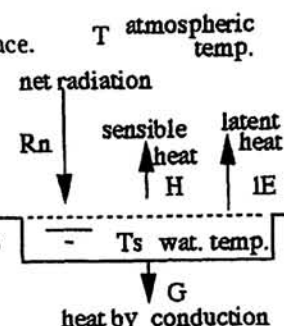$$So\downarrow = I_{00} (do/d)^2 \cos\theta \tag{5}$$

Fig. 1 Assumed System of heat balance.

* Dept. Chem. Eng., Shizuoka Univ., Hamamatsu, 432, Japan (Fax : +81·53·478·1173)

The term $L\downarrow$, long wave radiation from the atmosphere, is a function of temperature and humidity in the air, whereas the term σTs^4 represents long wave radiation from the surface.

$$L\downarrow = \sigma T^4 (a - b\,e^{1/2}) \qquad \text{Brunt equation} \qquad (6)$$

Two constants, a (=0.51) and b (=0.66) in this empirical equation, are called Yamamoto const.. The net radiation Rn is sensitive to the temperature of ground surface, and in general difficult to measure precisely, although it requires only one measuring instrument. On the other hand, $R\downarrow$ is relatively easier to measure correctly, but two measuring instruments (for $S\downarrow$ and $L\downarrow$) are necessary. For reference, example values in Eqs.(2) and (3) are shown below, units are all watt per square metre and surface albedo (ref) is assumed to be 0.1 :

	Atmospheric Temp.	σT^4	$S\downarrow$	$L\downarrow$	$R\downarrow$	$R\downarrow - \sigma T^4$
Daytime	20 ℃	419	700	295	925	506
Nighttime	10 ℃	365	0	285	285	-80

The two terms of heat transfer, sensible heat flux H and latent heat flux IE, are given as

$$H = h\,(\,Ts - T\,) \qquad (7)$$

$$IE = k\,(\,ew - e\,) \qquad (8)$$

The term h, heat transfer coefficient between the atmosphere and the surface, contains many error factors of measurement and difficult to estimate precisely. The term k, latent heat transfer coefficient, is a product of latent heat of water L and mass transfer coefficient k' which is easy to measure. The relation between h and k' at water-air system is known as the Lewis's relation :

$$h_{air} = k'_{air} \times (Cp)_{air} \qquad (9)$$

Thus, we measured the k' value experimentally and calculated h and k values.

Finally, the following equation is obtained by rearranging Eqs.(1) through (9) :

$$(d0/d)^2 \cos\theta\,(1-\text{ref})(\,1-\text{ref}\,)I_{00} + (0.51+0.066\,e^{1/2})\sigma T^4$$

$$= \sigma Ts^4 + 7.942(Ts - T) + 11.913(e_w - e) \qquad (10)$$

The equilibrium water temperature Ts can be estimated using this equation if all necessary data such as atmospheric temperature and humidity, solar radiation, etc. are given, and then, water evaporation rate can be calculated from the vapor pressure at the temperature.

Table 1. Example result of model calculation for temp., heat fluxes and evaporation rate.

Assumptions	Calculation results		
G = 0 (thermal insulation at the bottom)	equilibrium temperature	Ts	28.7 ℃
quasisteady-state (almost no wind)	sensible heat flux	H	28.9 w/m²
T = 21 ℃, rh = 0.5,	latent heat flux	IE	155.9 w/m²
$R\downarrow$ = 654 w/m² · $S\downarrow$ = 360 w/m²	evaporation rate	E	5.5 mm/day

Table 1 shows as an example a result of model calculation. In this case, more than 70% of the input solar radiation is converted into the long wave radiation from the surface, only about 25% is utilized for water evaporation. Using Eq.(10), we can estimate the steady state evaporation rate at any conditions. The model derived here, however, is still too simple to represent the real natural evaporation phenomenon. In the next step, an unsteady model will be developed with the effect of wind velocity on the mass/heat transfer coefficients and the presence of the clouds as well as all other necessary factors taken into account.

3. Numerical Model of Ascending Current by Thermal Convection

If the temperature of ground surface can be kept much higher than that of the surrounding atmosphere by absorbing solar radiation efficiently, it may be possible to create artificial

ascending current with least energy consumption. The possibility and feasibility of this concept can be examined by estimating quantitatively the following issues; e.g. how high the temperature can be increased, how far the ascending current can reach, how large area of black-body like ground surface should be required, what is the optimum shape and arrangement of the black-body like surface. The first problem belongs to the heat balance calculation discussed above. The others should be examined in terms of fluid mechanics by model simulation. Here, a simple model of two-dimensional, steady-state, natural convection on a finite-size, horizontal plate is supposed as a first step subject. The assumptions adopted in this study are as follows: 1) incompressible fluid with constant properties, 2) dry air condition, 3) a steady laminar flow, 4) Coriolis parameter force neglected, 5) Boussinesq approximation applied. Basic essential equations are simplified into the following forms :

Equation of continuity

$$\frac{\partial u}{\partial x} + \frac{\partial v}{\partial y} = 0 \tag{11}$$

Momentum equation

$$u\frac{\partial u}{\partial x} + v\frac{\partial u}{\partial y} = -\frac{1}{\rho}\frac{\partial p}{\partial x} + \gamma\frac{\partial^2 u}{\partial y^2} \tag{12}$$

$$0 = -\frac{1}{\rho}\frac{\partial p}{\partial y} + g\beta(T - T_0) \tag{13}$$

Equation of energy

$$u\frac{\partial T}{\partial x} + v\frac{\partial T}{\partial y} = \kappa\frac{\partial^2 T}{\partial y^2} \tag{14}$$

Equation of state

$$\rho = \rho_0\left\{1 - \frac{T - T_0}{T_0} + \frac{P - P_0}{P_0}\right\} \tag{15}$$

Boundary Conditions: $u = v = 0$, $T = T_0$ at $y = 0$ (16)
$u = 0$, $T = T_\infty$ at $y = \infty$ (17)

In order to obtain the solutions, a stream function ψ is introduced to transform the partial differential equations into a set of several simultaneous ordinary differential equations on the assumption that there exist similarity solutions . The stream function ψ is defined as ;

where

$$\psi = C \cdot v \cdot x^{3/5} \cdot f(\eta) \tag{18}$$

$$C = \left(\frac{g\beta(T_s - T_\infty)}{v^2}\right)^{1/5} \tag{19}$$

The similarity variable η is defined as

$$\eta = C \cdot \frac{y}{x^{2/5}} = G_r^{1/5} \cdot \frac{y}{x} \tag{20}$$

where

$$G_r = \frac{g\beta\Delta T x^3}{v^2} \tag{21}$$

in addition

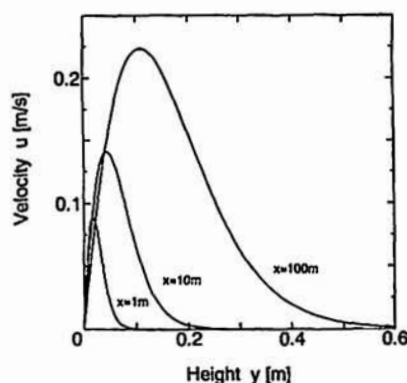$$\phi(\eta) = \frac{T - T_\infty}{T_s - T_\infty} \tag{22}$$

Fig. 2. Horizontal velocity profiles.

As seen above, all important variables are involved in the parameter Gr (Grashof number). Eqs.(11) through (15) can be reduced by a similar transformation to the following forms:

$$u = \frac{\partial \psi}{\partial y} = \frac{\partial \psi}{\partial \eta} \cdot \frac{\partial \eta}{\partial y} = C^2 v x^{1/5} f' \tag{23}$$

$$v = -\frac{\partial \psi}{\partial x} = -\left(\frac{\partial \psi}{\partial \eta} \cdot \frac{\partial \eta}{\partial x} + \frac{\partial \psi}{\partial x}\right) = \frac{1}{5}Cv\left(2Cx^{-4/5}yf' - 3x^{-2/5}f\right) \quad (24)$$

and

$$\frac{\partial u}{\partial y} = \frac{\partial}{\partial y}\left(C^2 vx^{1/5}f\right) = \frac{\partial \eta}{\partial y} \cdot \frac{\partial}{\partial \eta}\left(C^2 vx^{1/5}f\right) = C^3 vx^{1/5}f'' \quad (25)$$

As a result, we obtained the following ordinary differential equations and boundary conditions:

$$f''' + \frac{3}{5}f \cdot f'' + \frac{1}{5}f' \cdot f' + \frac{2}{5}\eta\phi' = 0 \quad (26)$$

$$\frac{1}{Pr}\phi' + \frac{3}{5}f\phi' = 0 \quad (27)$$

B.C. $f(0) = f'(0) = 0, \phi(0) = 1$ at $\eta = 0,$ (28)
$f'(\infty) = \phi(\infty) = 0$ at $\eta = \infty$ (29)

The integration of Eqs.(26) and (27) was carried out using Runge-Kutta-Gill method with Nachatsheim-Swigert Iteration Scheme. One of the simulation results is shown in Figs.2 through 4. Fig. 2 shows horizontal compensatory flow generated by ascending current. Size effect of the black body is clearly shown in both Figs.2 and 3 (temperature profiles along the height). Velocity vectors are illustrated in Fig. 4 in which approximate streamlines can be seen. The height of the ascending current seems to be about 6 times the width of the black body in this case. Thus, it is expected that real effective ascending current will be generated if a black-body like zone of several kilo meter square in size can be constructed.

4. Conclusion

A model which can represent the evaporation as well as the ascending current was constructed. In the future we will improve this model to simulate three dimensional, unsteady, more complicated phenomena.

——————— Nomenclature 2 ———————
Cp: constant-pressure heat capacity(J/mol K), E: evaporation rate (mm/day), Gr: Grashof number, P: atmospheric pressure(hPa), Po: air pressure at the ground surface(hPa), Pr: Prandtl number, Io∝ solar constant(w/m²), ref: albedo of the ground surface, ref: albedo of the atmosphere, rh: relative humidity of the air, do/dt ratio of distance between the sun and the earth, Rn: net radiation absorbed by the ground surface (w/m²), S↓: solar radiation at the ground surface (w/m²), So↓: solar radiation at the top of the atmosphere (w/m²), T: atmospheric temp., Ts: temp. of the surface at thermal equilibrium, ΔT: Ts $-$T∞., u: velocity in x-direction, v: velocity in y-direction, y; height(m), X: width of black body(m), β: coefficient of volumetric thermal expansion, η: similarity variable, θ: the zenith angle, κ: thermal diffusivity, ν: kinetic viscosity, ρ: density, σ: Stefan-Boltzmann const., Φ: dimensionless temp., ψ: stream function

——————— Nomenclature 1———————
e: vapor pressure (hPa), ew: saturation vapor pressure (hPa), g: gravitational acceleration (m/s²), G: heat flux by conduction(w/m²) h: sensible heat transfer coefficient (w/m² ℃), H: sensible heat flux (w/m²), IE: latent heat flux(w/m²), k: latent heat transfer coefficient (w/m² ℃), L↓: long wave radiation from the air(w/m²), R↓:total radiation to the ground surface(w/m²),
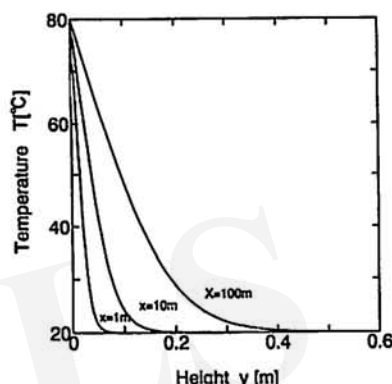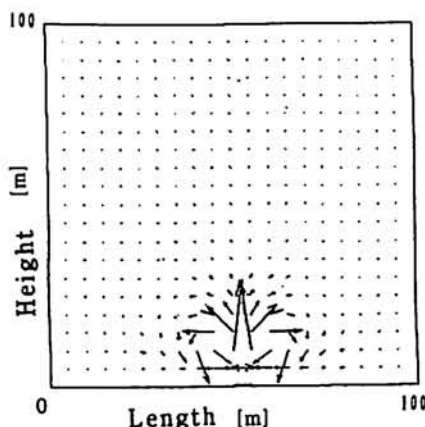

Fig. 3. Temperature profiles.

Fig. 4. Velocity vectors in X-Y direction.

Storing Water in Desert Against the Global Sea Level Rising

CHEN Qigao, LU Shixi, WEN Yongling

Abstract - The atmosphere is becoming warm, which would make the ice mountains to melt rapidly, the global sea level to rise, and many sea shores to be inundated. This disaster can be controlled or lessened by water storing in desert, whose advantages for mankind would be very great, for either controlling flood, or acquiring water sources to develop the desert. However, the engineering project is giant, it must gather the force in the world.

Key words: Underground water storing, Desert water storing, Surface water storing, Plants water storing, Air water storing.

1. Introduction

1.1 Effect of green house   In last decades the carbon dioxide in the atmosphere is increasing year after year. It will cause the concentration of carbon dioxide in atmosphere to reach a certain degree, and it can form the effect of green house for atmosphere. It is said that the consequences would be the ice mountains in the world to melt, the sea level would be rising, and a lot of land on the sea shores would be inundated. If this case would happened at once, it would cause a great disaster to all mankind. Therefore, all mankind must make most effort to stop this disaster happening.

1.2 Possibility of inundated disaster   At present the ratio of land area to the ocean area is about 0.414, it is said, as the land stores water of one meter depth, the sea level will decrease about 0.414 meter. In other words, as the land drain off one meter depth water, the level will increase about 0.414 meter. Therefore, water storing in large-scale can be used for lowering the sea level.

However, we must evaluate water quantity that would cause flooding disaster to how much degree. The main part of flooding water source is the ice accumulate in Antarctica and the mountains above the snow line, and the most dangerous is the water from the former.

The ratio of area of Antarctica to area of the land is 0.094. The glacier covers the area of the Antarctic about 93%. The air temperature is very low, the mean temperature in warmest month is below $0\,°C$. The mean depth of the glacier is about 1700 m.

If the ice on the Antarctica put on the land of the Earth, setting the correspondant ice depth on the Earth as x, we have the algebraic expression as follows:

$$1700 \text{ m} \times 0.094 = 1 \times x \qquad \text{then} \quad x = 159.8 \text{ m}$$

If the density of pressed snow is about 350 kg/m^3, as it melted into water, the water's depth h' would be:

$$h' = 159.8 \times 350 \div 1000 = 55.93 \text{ m}$$

which would be stored in the Ocean, the sea level would be rising up about the height h

$$h = 55.93 \times 29 \div 71 = 22.85 \text{ m}$$

It meant that the land below the sea level of height 22.85 m in these days would be inundated. Of course, this is just some tendency. Mankind should take some measures to protect the atmosphere environment, and to prevent from this disaster. The storing water in desert just is one of these efficient measures.

Dept. of Architecture, Chongqing Jianzhu University, Chongqing, Sichuan, China   630045

2. Water Storing

2.1 Water Storing in Underground Space Water storing in underground space is a general method, and in special case it has active meaning. The oil well can be poured with water, which is called the water lift recovery. This method has three advantages: the water can lift the oil layer up; the water, replacing oil to fill the underground space, can keep the rock body in stability; the water refill in oil well which can balance the water produced in combustion.

Therefore, the oil well should be refilled with water in order to protect the ground environment and the underground environment.

The oil wells or gas wells are very deep, but it can become shallow with refilling water.

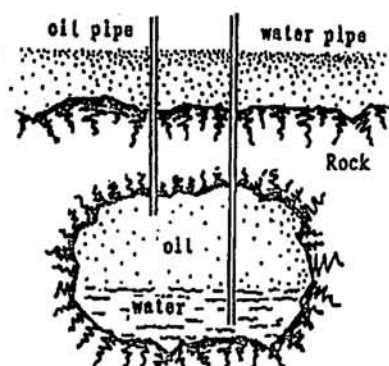The water-lift recovery is very good method for water storage.

Fig.1 Water lift recovery

2.2 Water Storing in Desert
2.2.1 Shifting sand bounded by water The land of desert is covered by the shifting sand, which has different thickness at different place above the original land forms. The shifting sand is very easy to move with wind, the configuration of land is changed very often. The shifting sand is very dangerous for human and animals, which would be buried under the shifting sand. If the shifting sand could be bounded by water, the conditions and the face of desert would be changed. Therefore, it is very important to store water in desert which is the first step against desertification.
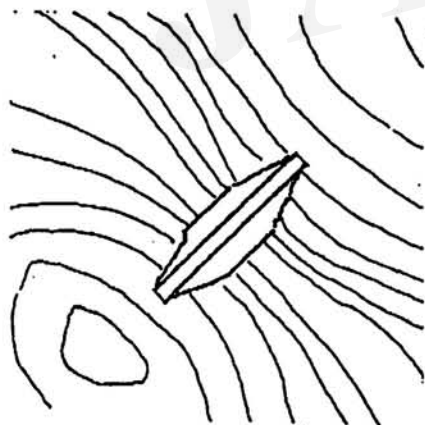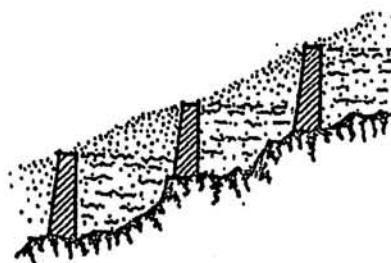

Fig. 2 Damming at gorge

Fig. 3 Damming along contour

2.2.2 The damming in desert

2.2.2.1 Damming at gorges Under the desert there are many mountains and valleys. The damming must be on the foundation rock at the gorge like the dam on a river. It can gather the water in the valley to form a reservoir (Figure 2).

2.2.2.2 Damming along contour As to the mountains, the dams should be constructed along the contour lines as shown in Figure 3.

The pores within the desert can store a great deal of water , so that the water running away would be stopped by a network of concrete dams as shown in Figure 2 and Figure 3.

The damming along the contours can form a group of terraced fields, so that the desert would be changed into oasis after the water storing.

2.3 Water storing in ground surface

2.3.1 The man-made lakes The topographical advantages are appropriated to build the lakes on ground surface. In desert reform there is a need of many man-made lakes, which can store a great deal of water, as well as control the local climate.

2.4 Water Storing in Plants

2.4.1 Reserved water in forest In plants is kept a great amount of water, which is divided two parts the free water and the chemical water.

· The free water is still water, which exists in and out of the plant bodies, such as, under the soil around roots. The water drops within leaves is called reserved water in plants.
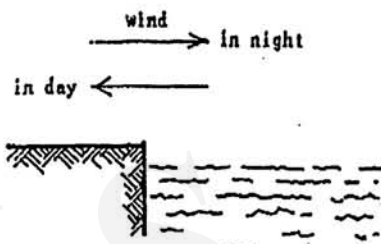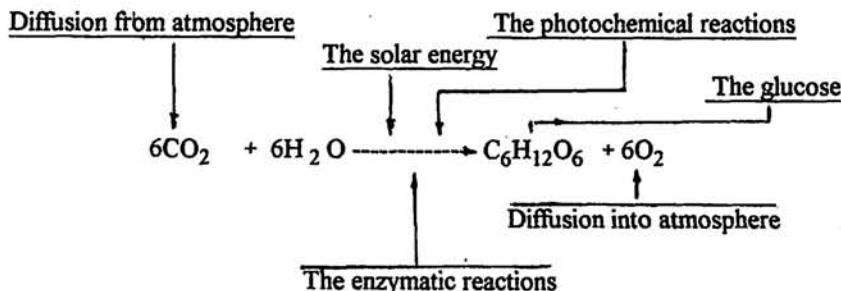
Fig. 4 Local wind on a bank

2.4.2 The chemical water The chemical water is the most important. It is fulfilled by plant photosynthesis with solar energy, carbon dioxide and water. Green plants are some integrated productive system. In the desert, the water is very lacking, of course, the yellow desert might be changed into green world by water storing.

Photosynthesis consists of three main processes, the photochemical reactions, the enzymatic reactions, and the diffusion. The overall processes can be summed up in the equation with mechanism

$$6CO_2 + 6H_2O \longrightarrow C_6H_{12}O_6 + 6O_2$$

In which carbon dioxide and water are combined to give glucose and oxygen thoroughly.

The enviroment and ecology benefits of photosynthesis by afforesting are presented as shown in Table 1 and Figure 5.

Table 1. Environmental and Ecology Benefits of photosynthesis

components	H_2O	CO_2	$C_6H_{12}O_2$	O_2
molecular number	6	6	1	6
molecular weight	18	44	116	32
amount	108	264	116	192
ratio of event to water	1	2.44	1.07	1.77
weight, ton	1	2.44	1.07	1.77

Fig. 5 afforesting benefits

From Table 1 it can be seen, using 1 ton of water and 2.44 tons of carbon dioxide can produce 1.07 tons of glucose and 1.77 tons of oxygen. The ecologic benefit is very good. The waste things are changed into good things, either store water or disposal CO_2, or produce O_2.
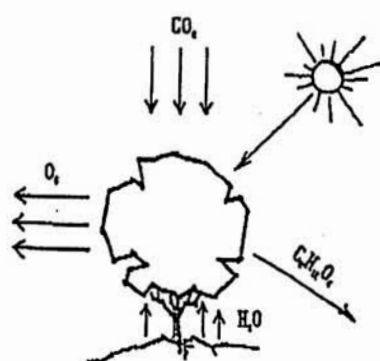
2.5 Water Storing in Air

In arid area, water or vapor in atmosphere is very low. As the desert stores water, forest would be developed, the cultivated land would be increasing also, water or water vapor in atmosphere would be richer, which is an inexorable trend and a consequence of afforesting.

However, water storing in air follows large-scale storing water in desert. In the process of changing the desert into green land, water vapor in the atmosphere can not reach to the degree of good weather, but it can be made in local place with such good weather. The solar green houses will be fitting to run against desertification in the beginning stage (Chen Qigao, Lu Shixi, Wen Yongling, 1993). The water is cyclically applied in the houses, the rain fall can replenish the stock in tree irrigating system, water in these systems is increasing day by day. The solar green house systems can assure to win the struggle to run against desertification.

3. Conclusions

Water storing in desert is one method to solve the environmental problem of the sea level rising. It is not only storing a great deal of water, but also using water to exploit desert, to afforest, and grow rice, plant crops, beans, melons, grass etc..

The afforesting and farming can absorb a good deal of water and carbon dioxide to produce oxygen and glucose which is unhydrous. After afforesting desert, trees, grass, flowers, and vegetables can be planted everywhere. The concentration of carbon dioxide in atmosphere will be lowered down. The reason of atmosphere temperature rising is controlled or cancelled out, the ice mountains on Antarctica can not break and melt, the sea level can not make notable change. It is very important for mankind to run against desertification.

References

Qu Gcping (1984), Environmental Problems and Stratcgy of China, China Environmental Scicnce Press, 1984, Beijing;

Margaret. L. Vickery (1984), Ecology of Tropical Plants, John With & Sons; Oxford;

Chen Qigao (1986), Energy Generation for Mankind by the Subsurface Space. The Preceding of International Symposium, Helsinki, Finland , pp 25-28, August 1986, Pregame Press, Oxford;

Chen Qigao, Lu Shixi, Wen Yongling (1993), Run Against Desertification, Desert Technology II, December 5-10, 1993, Hawaii.

Desalination Characteristics of Vapor Permeable Membrane for Irrigation

Masami Shiraishi*, Yoshiyuki Ohtsuka*, Hiroyuki Ii*, Takuji Nakamura*
Yoshihiko Hiraga**, Atsushi Tanigawa**

Abstract - Experiments were conducted to examine the fresh water production volume of the membrane using several thermal differentials. The average membrane permeability coefficient for these experiments for multiple tubes was 0.228l/hour/°C/m². As long as salinity levels remain below 10%, saline water can be reused without significant reduction in the fresh water production rate. The quality of the fresh water produced was extremely good for irrigation use. The thermal characteristics of subsurface soil were also investigated through experiments and two-dimensional numerical simulations of thermal conductivity.

Key Words: Desalination, Irrigation, Membrane, Saline Water

1. Introduction

Arid and semi-arid regions comprise one third of the land area on earth. Lack of water poses difficulties for agricultural development in such regions. The objective of this study is to investigate the possibility of securing additional supplies of fresh water for irrigation in these regions via the desalination of available saline water using vapor permeable membrane technology in conjunction with solar energy.

The proposed Saline water Irrigation System consists of irrigation tubes made of vapor permeable membrane matter. Saline water heated by solar energy runs through the tubes. The temperature difference between the heated water and the cooler soil medium produces water vapor which passes from the saline water through the surface of the membrane and condenses into fresh water in the soil. (Fig. 1)

2. Vapor Permeable Membrane

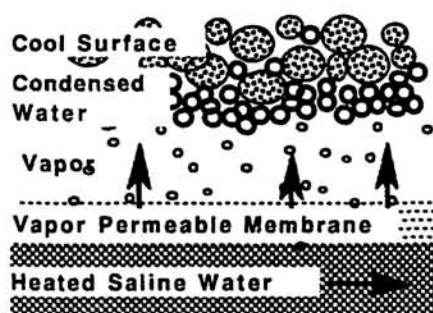The vapor permeable membrane is a fine porous membrane with hydrophobicity. The membrane was fabricated by expanding

Fig. 1 Distillation Process

---

* Institute of Technology, Shimizu Corporation (4-17 Etchujima 3, Koto-ku Tokyo 135 Fax : 81-3-3643-7260)
** Project Promotion Office, Kubota Corporation

polytetrafluoroethylene(PTFE), a kind of fluoropolymer which has good waterproof, moisture penetration, and release properties. It is also unaffected by oxidizing and reducing atmospheres, ultraviolet rays and common chemicals such as acids or alkalis. The membrane is widely applied to outdoor equipment as waterproof yet vapor permeable material. Table 1. shows general properties of the membrane.

Table 1. General characteristics of the membrane

Item	Description
Porosity	25~80%
Density	0.25~1.8 g/cm3
Max. Pore Size	0.5~5.0 micron (rely on porosity)
Thermal Stability	-240 ~ +270 ℃
Chemical Stability	Stable in acidity, alkalinity , organic solvent
Weather Resistance	Stable in ultraviolet rays
Hydrophilia	0 %
Stickiness	Non-stickiness and good release property

3. Experiment

To examine the membrane's distillation properties, we varied the experimental conditions at the experimental facility shown in Fig. 2, and measured the different volumes of fresh water produced. In the experiment, we pumped cool water through a normal polyethylene tube, and heated saline water through a vapor permeable membrane tube, which were combined in a multiple tube (Fig.3). Both the temperature and salt concentration ratio were varied as vapor pressure is dependent on these factors. We compared the volumes of fresh water produced at five different levels of salinity, i.e. 0%(city water), 3.5%, 7%, 10.5% and 14%, at several different temperatures. Saline water has limitations for circulatory use as the salt concentration gradually increases after each cycle, and the dissolved substances begin precipitating
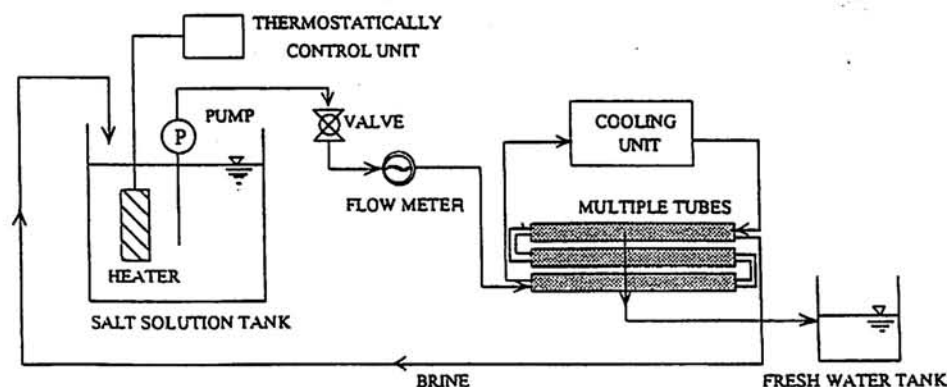

Fig.2 Flow Diagram of the Experimental Facility

at the 20% concentration level.

4. Thermal Analysis Model

In the past, we studied, through experimentation, the case of directly laying underground the vapor permeable membrane tube. This time, we further investigated the thermal characteristics of the soil surrounding submerged pipe by numerical simulations. Two-dimensional analysis for thermal conductivity was applied to the axial symmetric area at the center of the tube. Fig.4 shows a simplified model of the analysis area.

Primitive differential equation for heat transfer is given by

$$C\rho \frac{\partial \theta}{\partial t} = -\nabla(\lambda \nabla \theta)$$

$$= -\frac{\partial \theta}{\partial x}\left(\lambda \frac{\partial \theta}{\partial x}\right) - \frac{\partial \theta}{\partial y}\left(\lambda \frac{\partial \theta}{\partial y}\right)$$

Where λ is constant, above equation is modified to

$$= -\lambda \frac{\partial^2 \theta}{\partial x^2} - \lambda \frac{\partial^2 \theta}{\partial y^2}$$

Fig.3 Miltiple Tube

Fig. 4 Model of Analysis Area

Where θ : temperature [℃]
   c : specific heat [kcal/(kg・℃)]
   ρ : density [kg/m^3]
   λ : thermal conductivity [kcal/(m・h・℃)]

5. Results and Discussion

5.1 Multiple Tube Performance

Fig.5 showed the volume of fresh water produced corresponding to the difference in saturated vapor pressure between hot saline water and cooled water. The average membrane permeability coefficient for these experiments for the multiple tubes was 0.228 l/hour/℃/m². This value is about 50% less than the value for membrane tubes submerged in cool water. However, one meter of the multiple tube is able to supply 2.4 liters every six hours in operation. Electric conductivity of the produced
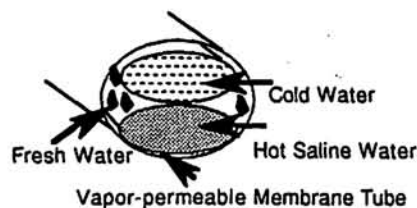
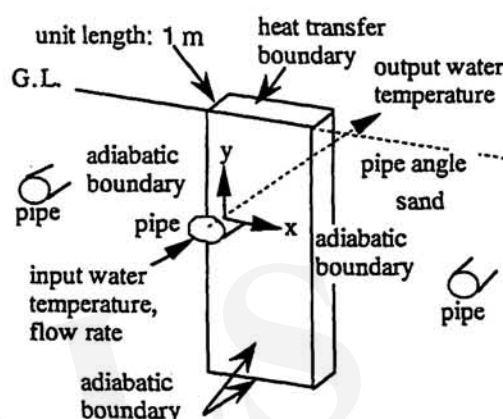water was 3.0-9.2 μS/cm. This result indicates that the water quality is extremely good for irrigation.

As shown in Fig.5, there were no significant differences in the volume of fresh water produced at the different salinity levels tested, except at 14%. This means that it is possible to continuously circulate saline water as long as its salinity remains less than 10%.
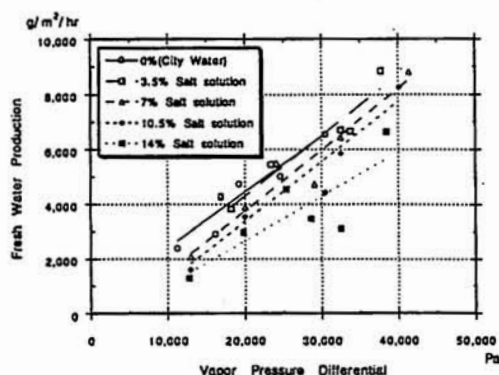

Fig.5 Comparison of Volume of Production Water Corresponding to Salinity Level

5.2 Temperature Profiles in Subsurface Soil

Fig.6 is a comparison of computed subsurface soil temperature profiles with experimental data at distances 1 cm and 3 cm away from the tube surface. In Fig.6, hot water was pumped through the tube for once every two hours, for one hour. Regarding the agreements after the first hour, calculated temperatures are 3-5℃ lower than the experimental data at each

Fig.6 Temperature Profiles

distance. These differences are probably due to the difficulty for the model in capturing changes of water content and soil temperature as water passes from the tube into the surrounding soil, affecting thermal conductivity and specific heat capacity. Latent heat transfer should be considered as well.
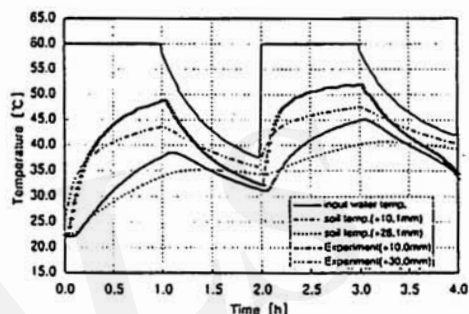
6. Conclusion

The proposed desalination/irrigation system of the study consists of irrigation tubes made of vapor permeable membrane matter. Experiments were conducted to examine the fresh water production volume of the membrane using several thermal differentials of the membrane tube. The multiple tube is efficient for irrigation from the viewpoint of water production volume and quality. The results of these experiments and simulations were used to design the pipe-laying, watering, and thermal balance arrangements of the system.

Reference

Ohtsuka,Y., Shiraishi,M., et al. (1994): Development of a Saline Water Irrigation System Using a Vapor Permeable Membrane, Journal of Arid Land Studies, 4, 7-13

Development of a Saline Water Irrigation System
Using a Vapor Permeable Membrane
(Experimental Cultivation)

Yoshihiko Hiraga[*], Atsushi[*] Tanigawa, Masao Yokota[**], Mitsuo Kubota[*],
Masami Shiraishi[***], Yoshiyuki Ohtsuka[***], Hiroyuki Ii[***]

Abstract – The Saline Water Irrigation System desalinates the saline water and
irrigates simultaneously, using a vapor permeable membrane(VPM). We carried
out experimental cultivation by two types of this system; subsurface and sur-
face irrigation. After we confirm efficiency of this system under the Japanese
climate, we calculate the operation schedule and projected irrigation volume
under the UAE climate.

Key Words: Saline water, Irrigation, Desalination, VPM, UAE.

1. INTRODUCTION

The purpose of the Saline Water Irrigation System is to carry out sa-
line water desalination and irrigation simultaneously, using a vapor
permeable membrane (VPM). We have confirmed through practical basic ex-
periments that the system is suited to irrigation.

We examined two types of this system; subsurface and surface irriga-
tion. The former type passes warm saline water into an underground VPM
tube and supplies the soil with fresh water that has been condensed from
vapor cooled by soil temperature.

The latter type utilizes a multiple tube. Multiple tubes are composed
of an outer tube, an internal VPM tube, and cold water polyethylene
tubes. In our setup, the multiple tubes are laid on the ground. Hot
and cold water was passes through the inner tubes from opposing or iden-
tical directions. In this structure, the vapor passing through the VPM
is cooled by the cold water and condenses on the outer tube in the form
of water droplets.

2. METHODS

Experimental cultivation was conducted with subsurface irrigation and
surface irrigation (multiple tube) under the following conditions:

Location: Greenhouse Ibaraki, Japan.
Cultivation bed: 3 sand cultivation beds(LxWxH= 6m x 0.6m x 0.3m)
Cultivated Crop: Komatsuma (brassica campestris var.)
Plots:(1) Subsurface irrigation.
      (2) Surface irrigation. Multiple tube with reverse water flow
        (hot water and cold water are passed in opposite directions).
      (3) Surface irrigation. Multiple tube with forward water flow
        (hot water and cold water are passed in the same direction).

In this experiment, service water was used as feed water and heated to
50°C through a heat exchange with hot water in a boiler, and the cold
water was cooled by circulating it through a passenger car radiator
placed outdoors. The pumps were driven for three 80 min. sessions per
day. Six irrigation tubes were buried 15cm below ground with 10cm spac-
ing between them, and three multiple tubes were laid on the surface with
20cm spacing. Fig. 1 shows the outline of the experiment.

[*] Water & Irrigation PT., KUBOTA Co., Tokyo 103 Japan (Fax:+81-3-3245-3300)
[**] Advanced Technologies Laboratoy. KUBOTA Co., Ibaraki 301 JAPAN
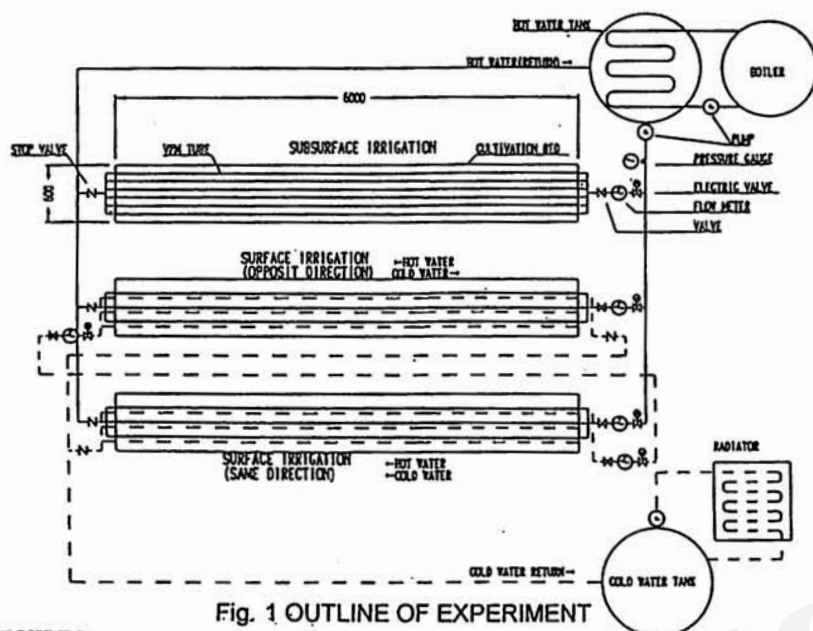[***] Institute of Technology, SHIMIZU Co., Tokyo 135 Japan

Fig. 1 OUTLINE OF EXPERIMENT

3. RESULTS

3.1 Subsurface Irrigation

As the water temperature inside the tube decreases due to heat conduction into the ground. Fig. 2 shows the temporal changes in the water temperature differential between upstream and downstream, and Fig.3 shows temporal changes in the soil temperature. The data from both figures was measured on Feb. 16, 1995, after completion of Komatsuna harvesting. The water temperature inside the tubes decreased during the operating hours by about $2°C$ after passing through the 6m long beds. At a depth of 15cm, the soil temperature showed a rapid increase within 30 min. after the start of operation, followed by a more moderate increase. After the cessation of operations, the temperature showed an initial rapid decrease followed by a more moderate decline. The surface temperature was relatively unaffected by the hot water inside the tube.
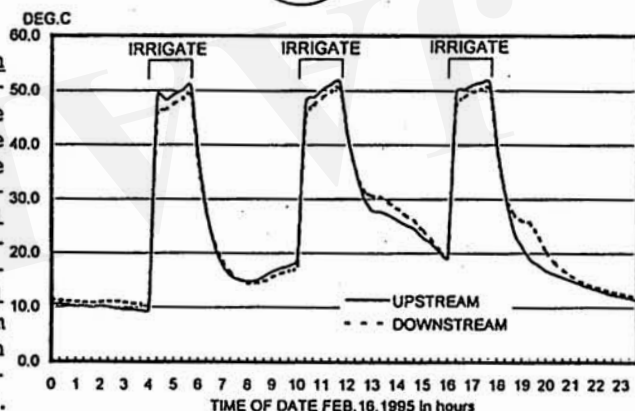

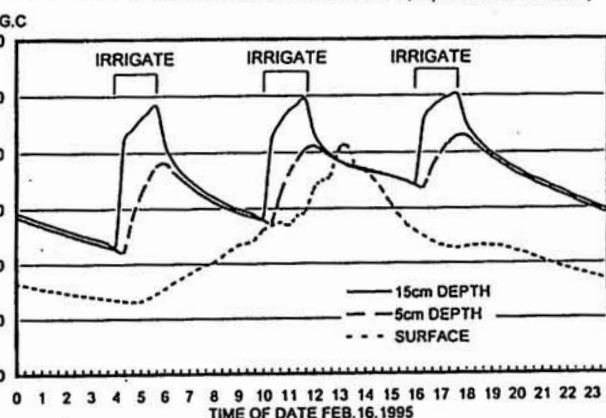Fig. 2 TEMPORAL CHANGES IN THE HOT WATER TEMP. (SUBSURFACE IRRIGATION)

Fig. 3 TEMPORAL CHANGES IN THE SOIL TEMP. (SUBSURFACE IRRIGATION)

Fig. 4 shows the yields translated into the figures per 10a. Each bar shows the yield for each bed section divided into lengths of 120cm each from the upstream to the downstream of the hot water. The Komatsuna harvested from the subsurface irrigation plot was inferior to that commercially available. It is assumed that the poor result was due to both the shortage of irrigation water and the adverse effects on the roots caused by the higher soil temperature from the hot water.

In a previous experiment using planters, however, the cultivation was successful. Countermeasures to prevent any future cultivation would be increasing the amount of irrigation water by burying tubes at shallower depths, widening the spaces between the tubes, and allowing roots to grow deeper (thus avoiding contact with the hot water).
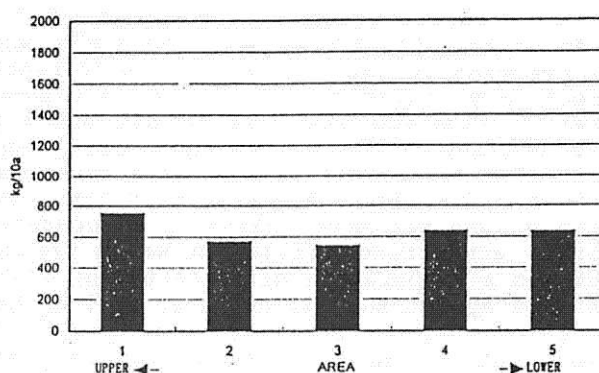

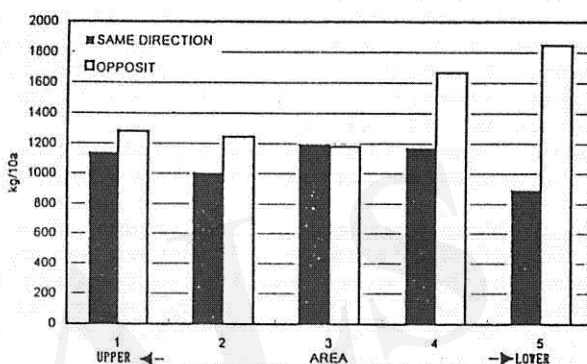Fig. 4 YIELDS BY THE SUBSURFACE IRRIGATION (KOMATSUNA)

Fig. 5 YEILDS BY SURFACE IRRIGATION (KOMATSUNA)

3.2 Surface Irrigation Fig. 5 shows the yields by surface irrigation. The surface irrigation resulted in a harvest of Komatsuna which was almost of the same quality as commercially produced. The cultivation beds with multiple tubes in which hot and cold water was passed in opposite directions had slightly higher yields than beds with water passed in the same direction. The bed area downstream from the hot water tended to have higher yields when water was passed in opposite directions. Whether or not these results are within experimental tolerance cannot be judged from this single experimental cultivation.

4. CONSIDERATIONS

So far we have carried out experiments to develop this system and can confirm its efficiency for cultivation under the climate of Japan. Here we calculate the operation schedule and projected irrigation volume using the climate data in Abu Dhabi, UAE.

4.1 Subsurface irrigation The membrane's water producing capacity in subsurface irrigation is determined by the relation between hot water

Table 1. The operation plan of the subsurface irrigation system

	Summer(Aug.)	Winter(Jan.)
T1	70 C	50 C
T2	37 C	22 C
Qn	7mm/day	3mm/day
q	0.62mm/hr or more	0.62mm/hr or more
R	6hr (12 times) or less	2.5hr(5times) or less

T1: Hot water temp.
T2: Soil temp.
Qn: Required irrigation water
q: Projection of irrigation water per session (30min)
R: Operation time per day

and soil temperatures. As a result of the domestic experiments conducted so far, the capacity was $900g/m^2/h$ when the hot water temperature, soil temperature, and temperature differential were $50°C$, $20°C$ and $30°C$, respectively. Furthermore, it can be assumed from the domestic experimental cultivation that the actual water production persists for the first 30 minutes or so from the initial input of hot water because the subsurface flow of hot saline water causes a rapid increase in soil temperature. Therefore, the operation time can be determined and the irrigation volume projected assuming an operation time is 30 minutes and a membrane subsurface irrigation water producing capacity of $900g/m^2/run$ (provided a temperature differential of $30°C$ is realized).

In this system the saline water will be heated by solar energy. It is calculated that the hot water will be $70°C$ during summer (Aug.) and $50°C$ during winter (Jan.). Also it can be postulated that the temperature differential would be almost $30°C$, since the soil temperature data measured at a depth of 10cm (where the tubes will be buried) in Bateen, Abu Dhabi (1994) show that it is $21.4°C$ in Jan. and $36.8°C$ in Aug.

The required irrigation water can be calculated using the weather conditions. Assuming the cultivation to be carried out in a net house, the water requirement could be estimated to be a maximum of 7mm/day in Aug. and a minimum of 3mm/day in Jan.

Table 1 shows the operation plan of the subsurface irrigation system and the projected irrigation volume given these assumptions.

4.2 Surface Irrigation The volume of water produced by the multiple tube in surface irrigation is determined by the temperature differential between the hot water and the surrounding area (which is cooled by the cold water tube). The following empirical formula shows the membrane's water production capacity. It basis the domestic experiments conducted so far, and the VPM tube is directly cooled by water in the case.

$Y = 0.994X$ ..... Formula 1
Where:
- Y : Water production capacity per unit area of membrane $(L/m^2/h)$
- X : The vapor pressure differential between the VPM and the surrounding area (kPa).

Table 2 shows the irrigation volume and the operation time derived from the calculation. Since the cold water temperature is equal to that of the groundwater, it was assumed to be constant at $35°C$. The irrigation volume is the figure obtained in the case of laying the three multiple tubes laid in the cultivation beds.

Table 2. The operation plan of the surface irrigation system

	Summer(Aug.)	Winter(Jan.)
T1	70 C	50 C
T2	35 C	35 C
Qn	7mm/day	3mm/day
q	3.4mm/hr or more	2.3mm/hr or more
R	2.1hr	1.3hr

T1: Hot water temp.
T3: Cold water temp.
Qn: Required irrigation water
q: Projection of irrigation water per session (30min)
R: Operation time per day

However, the tube's water production capacity used for these calculations is a figure obtained from an indoor experiment, so a validation test is necessary to confirm under actual desert conditions.

Reference
Ohtsuka, Y. et al. (1994):Journal of Arid Land Studies, 4:7-13.
FAO (1977):FAO Irrigation and drainage paper, 24.

Aral Sea desertification caused by irrigation and its effects on water quality

Yoshiko KAWABATA*, Hiroyuki NAKAHARA*, Kazuo NISHIMURA*,
Norio ISHIDA*, Hiroto MAEDA**, Yukio KATAYAMA* and Tsuneo TSUKATANI***

Abstract - A survey was conducted to compare the chemical properties of water, pore water, and sediment from the Small Aral Sea, the Lake Chardara, the Lake Kamyslybas, and the Syr-Darya. The pH, EC, major ions, and alkalinity were measured. In the northern part of Small Aral Sea (AR-1), major ions, alkalinity, pH, and EC in the water were higher than other points. However, the major cations precipitated in the sediment were lower than other points. The concentrations of sodium, potassium, and chlorine in AR-1 were less than those in seas water, but calcium, magnesium, and sulfate ion were higher.

Key words : Aral Sea, saline lake, chemical composition, pore water, sediment,

1. Introduction

The Aral Sea is a big closed lake located in the arid area of Central Asia. It follows that the water level of the Aral Sea was heavily depended on the amount of water contributed by two major tributaries, the Amu-Darya and the Syr-Darya. In the past 30 years, it was the world's fourth largest lake in area. However, its area has decreased rapidly and its water salinity have become high. The decrease in the area was caused by the large scale irrigated agriculture which started in 1950's. This resulted to the marked diminution of water inflow from the Amu-Darya and the Syr-Darya. Most part of the dried bottom of the Aral Sea became a sandy desert. The serious problem is the blowing of sand and salt from the dried bottom.

Therefore, this research was conducted for the evaluating changes in water and sediment qualities at the different locations of these water bodies.

2. Materials and Methods

This research was conducted in the Small Aral Sea, Lake Kamyslybas, Lake Chardara, and the Syr-Darya on August and September 1994 (Fig.1). Lake Kamyslybas was formed by connecting pond in the floodplain and Syr-Darya. Lake Chardara was formed by damming of Syr-Darya. Water and sediment core samples were collected in these study areas. The water quality such as pH, EC, DO, and temperature were also monitored during field survey. The water samples were filtered through 0.45-μm Millipore filters immediately for element analyses. The core samples were

* Fac.of Agr.,Kyoto Univ., Kyoto 606-01, Japan,(Fax:+81-75-753-6375)
** Fac.of Fish., Kagoshima Univ., Kagoshima 890,Japan
*** Kyoto Economical Institute, Kyoto Univ., Kyoto 606-01, Japan
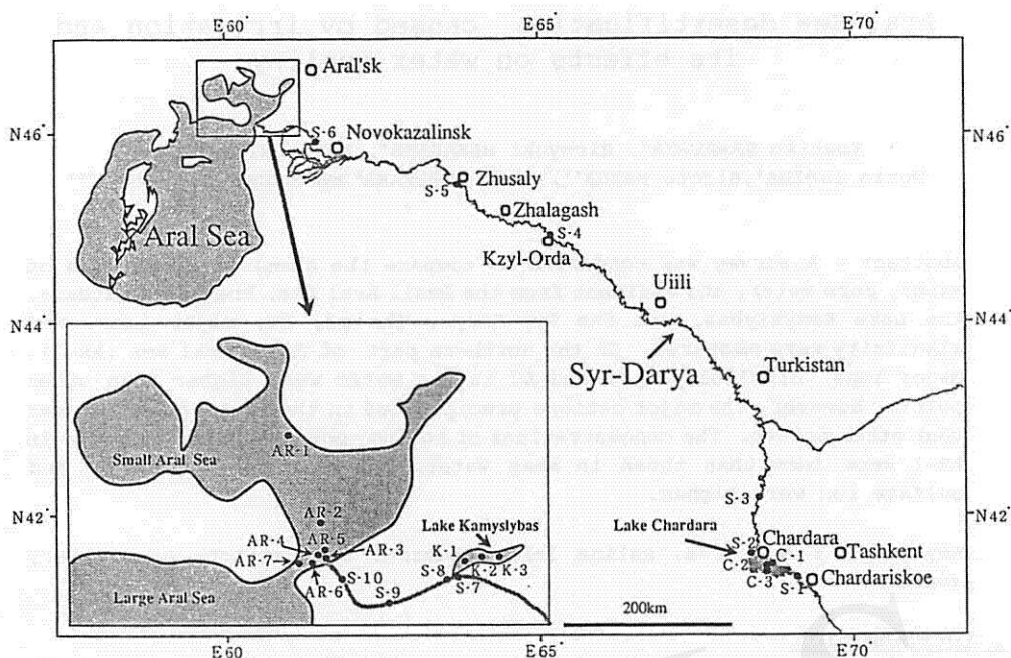
Fig.1   Location of study areas

sectioned at 2cm intervals. The pore waters of each depth of sediment were collected from sediment using a centrifuge. Then, sodium, potassium, calcium, and magnesium in water and pore water samples were determined by a atomic absorption spectrophotometry.   Chlorine was determined by a spectrophotometry method with mercury thiocyanate. Sulfate ion was measured by a turbidimetry method with barium chloride. Alkalinity was determined by a titration method.   Sediments were dried at 50°C and were subjected to instrumental neutron activation analysis (INAA) for determination of sodium, potassium, calcium, and magnesium.

3. Results and Discussion

The pH, EC, DO, temperature, and major ions in water from the Small Aral Sea, the Lake Kamyslybas, the Lake Chardara, and the Syr-Darya are shown in Table 1.   The pH values of water in these areas were almost same.   The EC values in the Syr-Darya, the Lake Chardara, and southern part of the Small Aral Sea were low.   The EC in the Small Aral Sea are increased forward the north direction.   In the Small Aral Sea, the turbid water from Syr-Darya flows into the southern part of the Small Aral Sea and then the mixed water flow into the Large Aral Sea.   The EC values in the Lake Kamyslybas are almost the same as in AR-4.   The EC values in the Small Aral Sea show that the water quality of Syr-Darya does not influence the water in the north part in the Small Aral Sea.

The concentrations of sodium, potassium, calcium, and magnesium,

Table 1. Locality details and physico-chemical parameters from Syr-Darya, Lake Chardara., Lake Kamyslybas, and Small Aral Sea

Name	Position		pH	EC	DO	Temp.	Na$^+$	K$^+$	Ca^{2+}	Mg^{2+}	SO$_4^{2-}$	Cl$^-$	alkalinity
	Lat. N	Long. E		(mS/cm)	(mg/L)	(°C)	(meq.)	(meq.)	(meq.)	(meq.)	(meq.)	(meq.)	(meq.)
C-1	41° 12'41.6"	68° 09'53.2"	8.47	1.54	8.3	25.1	5.8	0.1	5.5	5.2	11.6	2.5	2.6
C-2	41° 09'02.2"	68° 25'17.1"	8.34	1.66	7.6	22.2	5.8	0.1	5.7	5.3	12.0	3.8	2.4
C-3	41° 06'57.3"	68° 25'17.1"	8.58	1.25	6.3	21.6	4.3	0.1	4.1	3.8	8.4	2.0	2.2
S-1	41° 06'57.3"	68° 25'17.1"	8.17	1.72	7.2	25.7	6.2	0.1	7.3	5.7	13.0	2.8	4.8
S-2	41° 14'55.0"	67° 57'58.7"	8.18	1.47	4.9	22.8	4.9	0.1	4.7	4.7	10.0	2.3	2.0
S-3	42° 12'54.4"	68° 14'35.6"	8.52	1.47	7.0	25.7	5.5	0.1	5.0	5.1	10.7	2.6	2.4
S-4	44° 45'50.7"	64° 31'52.9"	8.43	1.62	8.7	18.4	5.2	0.1	4.6	4.7	10.3	2.8	3.0
S-5	45° 28'15.3"	65° 03'44.5"	8.51	1.56	7.7	20.2	5.8	0.1	5.0	5.3	10.7	2.8	2.6
S-6	45° 45'30.0"	62° 19'52.9"	8.51	1.46	6.3	20.2	5.5	0.1	4.9	5.1	10.2	2.5	2.2
S-7	46° 05'28.9"	61° 32'54.5"	8.47	1.60	7.3	17.6	5.5	0.1	5.3	4.8	10.3	2.8	2.4
S-8	46° 06'69.6"	61° 29'68.0"	8.36	1.59	9.2	16.5	6.1	0.1	5.5	5.7	12.0	3.0	2.4
S-9	46° 15'46.1"	61° 16'11.6"	8.21	1.54	—	18.4	6.0	0.1	4.8	5.5	12.0	2.8	2.6
S-10	46° 05'70.6"	61° 53'47.0"	8.16	1.67	7.0	15.7	6.6	0.1	5.2	5.8	11.4	3.0	2.6
K-1	46° 09'15.0"	61° 41'70.5"	8.48	11.1	6.9	18.7	35.0	0.7	13.5	28.2	52.0	20.0	3.0
K-2	46° 09'22.1"	61° 45'18.6"	8.49	11.2	9.0	18.4	47.2	0.9	18.2	35.6	68.8	26.3	3.6
K-3	46° 10'37.1"	61° 53'46.6"	8.32	11.4	9.3	18.2	46.4	0.9	18.1	36.3	63.7	25.7	3.6
AR-1	46° 47'08.3"	61° 39'89.1"	8.61	44.1	9.6	17.1	246.7	7.5	135.5	122.2	162.4	256.6	4.4
AR-2	46° 12'23.1"	60° 51'57.6"	8.45	29.4	7.3	17.4	150.7	4.4	23.3	72.8	104.3	147.6	3.6
AR-3	46° 08'13.6"	60° 49'463"	8.19	1.62	7.8	17.2	6.6	0.1	5.3	5.9	12.2	3.0	2.4
AR-4	46° 08'39.6"	60° 49'19.5"	8.45	15.4	7.8	16.7	80.9	2.3	15.0	40.3	52.0	78.8	3.0
AR-5	46° 08'63.0"	60° 19'29.0"	8.46	29.7	6.9	14.4	141.1	4.1	21.8	68.8	90.9	140.4	3.4
AR-6	46° 06'62.8"	60° 49'30.6"	8.35	2.25	7.8	21.1	10.7	1.4	6.0	7.8	16.1	7.6	2.6
AR-7	46° 05'87.3"	60° 44'16.6"	8.50	13.0	8.9	20.7	68.4	0.1	11.0	35.5	54.8	62.1	2.8

chlorine, and sulfate ion in the water increased within the Small Aral Sea. However, the concentrations of alkalinity show only small variability in these area. The dramatically high concentrations in AR-1 could result from evaporation of the water and not due to mixing within the Small Aral Sea.

The major cation concentrations of water are compared with those of pore water, and sediment (Fig. 2). The variations in the concentrations of alkali metal such as sodium and potassium in water and pore water have the same profiles each other, but in the case of alkali-earth metal such as calcium and magnesium the profiles are different. Especially, the concentrations of sodium, potassium, calcium, and magnesium in sediment on AR-1 is lower than other sites.

Table 2. The concentrations of major ions of sea water, Aral Sea in 1965 from Aladin, and AR-1

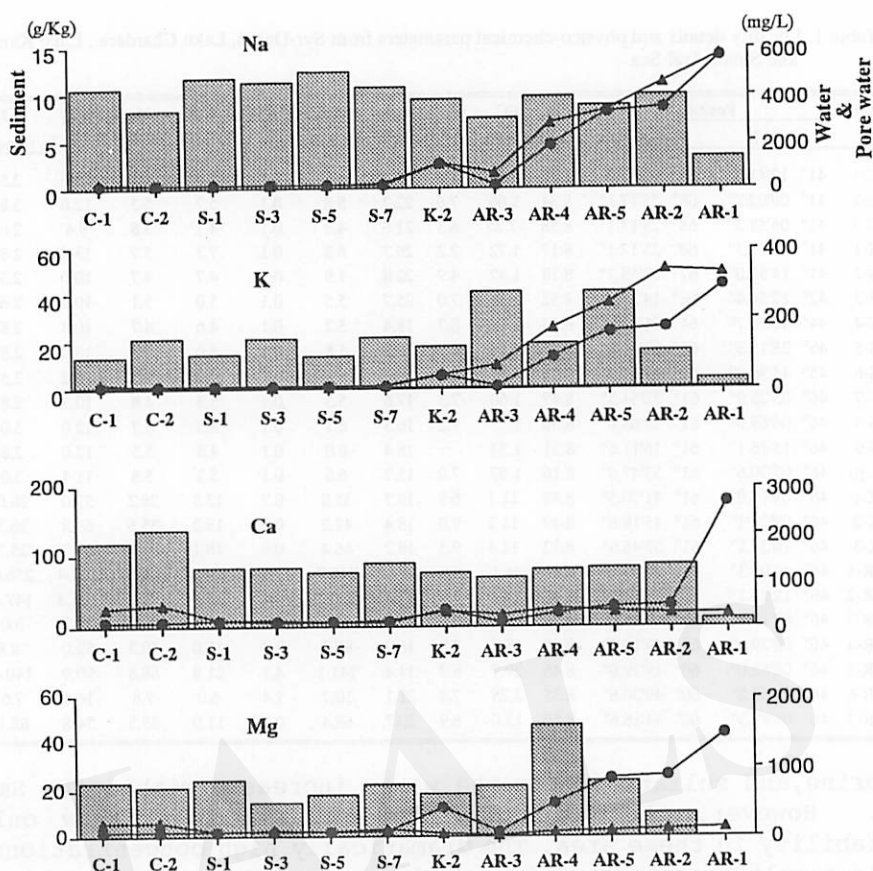|	Na$^+$ (meq.)	K$^+$ (meq.)	Ca^{2+} (meq.)	Mg^{2+} (meq.)	SO$_4^{2-}$ (meq.)	Cl$^-$ (meq.)	HCO$_3^-$ (meq.)
Sea Water	459.9	9.7	20.0	104.6	55.2	535.3	2.3
Aral Sea(1965)	104.4	2.2	22.8	48.2	69.6	215.4	0.8
							alkalinity
AR-1(1994)	246.7	7.5	135.5	122.2	162.4	256.6	4.4

Fig. 2. The concentrations of cations between water, pore water, and sediment
from Lake Chardara(C), Syr Darya(S), Lake Kamslybas(K), and Aral Sea(AR).
Plots are based on mg/L of individual ions of water calculated from Table 1.

● Water   ▲ Pore water   ▨ Sediment

The major cation concentrations of water in AR-1 are compared with sea water and the water of the Aral Sea in 1965(Table 2.). The concentrations of sodium, potassium, and chlorine in AR-1 were less than those in sea water, but the concentrations of calcium, magnesium, and sulfate ion were higher. The major ion concentrations in AR-1 were higher than those of the Aral Sea in 1965. Especially, the calcium concentration in AR-1 was higher than that of the Aral Sea in 1965.

These mechanisms are not known, but the increases of those ions in this sites were caused by the large scale irrigated agriculture. The area of the Aral Sea will decrease and the desertification will be continued, unless the large scale irrigated agriculture will be stopped.

Reference

Aladin, N.V. and Potts, W.T.W. (1992) : Changes in the Aral Sea ecosystems during the period 1960-1990 : Hydrobiologia 237: 67-79

The Effect of Forestation on a Shallow Groundwater Reservoir in an Arid Sand Dune Terrain

Eilon. M. ADAR*, Israel. GEV*, Pedro BERLINER* & Arie. S. ISSAR*

Abstract - Forestation and reforestation in an arid sand dune terrain raise the issue to what extent it affects the local groundwater system: that is, transpiration versus groundwater recharge. In arid basins sand dunes are considered to be the most efficient zones for groundwater recharge. Infiltration and deep percolation over sandy deserts are thought as the fastest source of aquifer replenishment. Therefore, forestation and the associated transpiration may affect local groundwater recharge. Tamarisk forest, one of the most popular species that has been successfully adopted to an arid sand dune terrain, was used to examine the source of the transpired water: soil water versus shallow groundwater. Stable isotopes of oxygen-18 and deuterium were employed to identify and to quantify the relative contribution of water utilized in the process of transpiration.

Key Words: Forestation, Groundwater recharge, Stable isotopes, Sand dunes.

1. Introduction

Reforestation in sand dune terrain is well established practice. The dunes are not only stabilized but also utilized as productive land for timber and firewood.. A combination of high infiltration rate and low water-holding capacity infers fast, deep percolation, which is related to groundwater recharge. However, due to the high rate of effective pores and high top-soil temperatures, potential diffusion of vapors also implies a high rate of soil evaporation. Though the amount of rainfall is small, a relatively high percentage reaches the local aquifer.

Therefore, when trees are introduced into sand dunes, one has to consider how this interferes with the local water balance and how it will affect the groundwater reservoir, through the rate and magnitude of recharge. These aspects have been studied in a small forest of tamarisk trees which was planted in the late forties and in the early fifties over sand dunes in the northern Negev desert, Israel. Shallow groundwater was found 15 to 17 meters below surface.

The tamarisk trees like many other desert plants are known to have a dual root system: shallow roots within the top sand, and deep roots just above the saturated water table. Tamarisk roots were found at the top 2 m of the sand, and within the shallow aquifer 16 m below surface

As $\delta^{18}O$ and δD composition in soil water were found to be significantly different than in groundwater, the distribution of $\delta^{18}O$ and δD composition in the topsoil and in groundwater were related to the spatial isotopic distribution along 15 m of double root system, stem flow, and twigs of two Tamarisk trees. For all practical purposes, in the process water withdrawal from the soil matrix into the roots, the isotopic composition of both oxygen-18 and deuterium do not go through any isotopic fractionation. Therefore, these isotopes can be used as conservative tracers along the flow pass during transpiration. This concept was studied and tested in a single isolated tree that its roots were exposed down to 12 m below surface in a nearby sand quarry (Adar et al., 1995). In that experiment we examined the hypothesis that (a) the sap flow in the trunk maintains the isotopic values as in groundwater; and (b) that the liquid in the top root system represent the isotopic composition of the top soil moisture. The same isotopic composition in groundwater were traced in the deep root system and along the main root (trunk) connecting the lower roots with the top roots. Above the confluence, in the stem, branches and twigs the isotopic composition was found to be a mixture of relatively depleted groundwater with enriched isotopes in the top soil water. (Gev, 1995). The aforementioned findings hold as long the water from the core wood were extracted from the xylem only. While the xylem carry the transpired fluxes, the phloem contains liquid that went through a significant enrichment in the stomata.

* The Jacob Blaustein Institute for Desert Research, and Department of Geology and Mineralogy, Ben-Gurion University of the Negev, Sede Boker Campus 84990, Israel (Fax: +972-7-557042)

Having the technology to measure the transpired fluxes and the isotopic composition in the stem, enables to calculate the relative contribution of soil and ground water providing the isotopic composition is known in the subsurface sources. The main research objective was to determine the relative role of soil water versus shallow groundwater as sources for transpiration.

2. Methods

Three sets of sap water was extracted by azeotropic and vacuum distillation from twigs, and from the xylem taken from a stem core 0.5 m above the surface. Cores of wood from the tamarisk tree were taken from the main trunk, stem, and main branches where the xylem was separated immediately from the phloem into sealed vials. The coreholes were then filled and sealed with silicon to prevent damage to the tree. Thin roots from the upper root system were also sampled for water extraction. The temporal isotopic distribution were measured along top soil profiles with a calibrated neutron moisture detector. Top soil moisture was extracted by azeotropic distillation from auger sampler taken every 20 to 30 cm taken in the vicinity of the tree on the same day to compare with that obtained from the thin roots. Local groundwater were periodically sampled in an observation well 10 m from the tested trees.

Total sap flow through the stem is equivalent to the amount of water utilized by the tree for transpiration. Sap flow was determined using the calibrated heat pulse method for flux measurement in the stem (Cohen *et al.*, 1981). The method relies on measuring the convective velocity of heat wave that assumed to represent the advective flux

3. Theory

Assessing the relative portion of groundwater in the total rate of transpiration relies on the fact that both soil moisture and groundwater are mixed in the sap flow passing though the stem. Also, due to intensive evaporation, the isotopic composition of soil moisture is significantly enriched in heavy isotopes as opposed to that of local shallow groundwater.

The total rate of transpiration from the canopy "Tr" is equal to the rate of sap flow through the stem (st), which is combined from water extracted from soil moisture V_s and groundwater V_{gw}. Similarly, the isotopic composition of the liquid passing through the stem C_{st} is a linear combination of the average isotopic value in soil moisture C_s and in groundwater C_{gw}. A simple isotopic mass balance approach implies the following expression:

$$Tr_{st} C_{st} = Vs C_s + V_{gw} C_{gw}. \tag{1}$$

Therefore, for $\delta^{18}O$ and δD one obtains a set of two mass balance equations with Vs and Vgw as the only unknowns.

$$Tr_{st}\, \delta^{18}O = Vs\, \delta^{18}O_s + V_{gw}\, \delta^{18}O_{gw}$$

$$Tr_{st}\, \delta D = Vs\, \delta D_s + V_{gw}\, \delta D_{gw}. \tag{2}$$

For a particular observation the measured rate of sap flow (Tr_{st}) and the isotopic composition of groundwater are quite constant. However, the $\delta^{18}O$ and δD values vary along the top soil profile. Therefore, the accurate composition of moisture entering and dominating the isotopic composition of the upper root system is not precisely known. The average values for $\delta^{18}O$ and $\delta^{18}D$ in the top soil layer were taken as the representative values for the upper root system along the two meters of soil profile. In the following, the isotopic values of the xylem sampled from the stem are also average values of several Tamarisk trees situated around the observation holes.
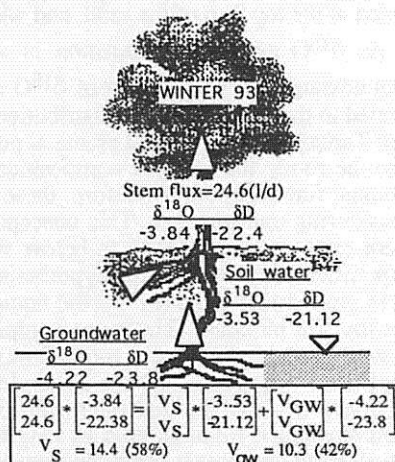

Fig. 1 Stable isotopes distribution and calculated fluxes from ground water and soil moisture in winter 1993.

3. Observations and results

Results from the forested area for winter 1993 are presented in Fig. 1. During January 1993, the soil moisture content was 98 mm along 2 m of the top sand (mm/2m), and the rate of sap flow was 24.6 lit./day) (Adar et al., 1995). In this month the soil moisture contribution to the total sap flow was 14.4 lit./day (58%) compared to only 19.3 lit./day (42%) from groundwater.

Fig. 2 presents the results from the second set sampled in mid April. The rate of transpiration was slightly higher and reached an average value of 27.2 liters per day. The total top soil moisture content was 96.7 mm/2m, similar to that found in the winter. Groundwater content dropped, however, by 14 cm (Gev, 1995). Solving the isotopes mass balance equations for V_s & V_{gw} revealed that in this month the soil moisture contribution to the total sap flow decreased to 8.74 lit./day (32%) with 18.42 lit./day (68%) from groundwater.

Fig 3 illustrates the $\delta^{18}O$ and $\delta^{18}D$ distribution in August 1993. The top soil moisture content dropped to 74 mm/2m. Though the deep roots obviously reached groundwater, the average daily transpiration, as measured by heat pulse method in the tamarisk stems, was only 9.34 lit./day. Solving Eq. (2) for V_s and V_{gw} revealed 3.81 (41%) and 5.53 lit/day (59%) from soil moisture and groundwater respectively.

Fig. 2 Stable isotopes distribution and calculated fluxes from groundwater and soil moisture in spring 1993.

Fig. 3 Stable isotopes distribution and calculated fluxes from groundwater and soil moisture in summer 1993.

4. Discussion

During three years of hydrological study in this region (Gev, 1995), we have gathered evidences from 16 soil profiles in which the isotopic composition of the soil moisture was always significantly enriched relative to the local shallow groundwater. As expected, that was reflected in the isotopic values in the sap flow in both upper and lower roots systems when the water was extracted from the xylem only.

For the three tests, groundwater, though it is at least 16 m below the surface, always serves as the major source of transpiration. In view of winter versus spring and summer results, the rate of transpiration during spring time increased due to climatic conditions though the topsoil moisture remained almost the same. Thus, the lower root system became more active in extracting water from the shallow aquifer (42% in January versus 68% in April). This was also associated with a 14 cm decrease in local groundwater level (Gev, 1995). During the summer, the transpiration rate decreased dramatically to 9.34 liters/day. As soil moisture content at the upper root system also decreased from

97 to 74 mm/2m, the relative contribution of soil water to the total rate of transpiration increased from 32% to 41%.

The fact that groundwater serve as the major source for transpiration might be attributed to the fact that the total hydraulic potential required to lift groundwater to the surface is still lower than to extract soil moisture. High soil water matrix potential (affected mainly by the content of water and clay) and high soil water salinity that affects the osmotic potential across the roots membrane, impose higher energy level for the extraction of soil water versus groundwater. This issue has not yet been confirmed and it is suggested for a future common research with botanist, soil physicist and hydrologist.

Results indicate the applicability of utilizing of stable isotopes to elaborate on the relative rate of water extraction by each root system. However, since $\delta^{18}O$ and δD values vary along the soil moisture profile, the accurate composition of moisture entering and dominating the isotopic composition of the upper root system is not precisely known. It might also be that each ring in the xylem is dominated by sap flow originating at a specific root section with different isotopic values.

Therefore, one xylem sample from the stem taken for $\delta^{18}O$ and δD analyses might not represent the accurate isotopic composition of the transpired fluxes. These inaccuracies might impose some uncertainties into the model which decreases the precision of the assessed fluxes.

As groundwater replenishment is concerned, mature Tamarisk trees extract both soil and ground water. A comprehensive study of the hydrological balance of a forested area and bare sands (Gev, 1995) suggests that forestation with Tamarisk trees does not decrease radically the local groundwater recharge. Most of the soil water in the forested area is protected from direct evaporation by the canopy and mainly by the thick mulch. Without trees, most of the soil moisture that is available for transpiration would be evaporated and would not reach the local aquifer.

References

Adar, E. M., I. Gev, J. Lipp, D. Yakir, J. Gat and Y. Cohen (1995). "Utilization of oxygen-18 & deuterium in stem flow for the identification of transpiration sources: Soil water versus groundwater in sand dune terrain". in The First International Symposium on Application of Tracers in Arid Zone Hydrology, August 22-26, 1994 Vienna, Austria. IAHS Pub. No. 232 (in press).

Cohen, Y., Fuchs, M., and Green, G.C. 1981. Improvement of the heat pulse method for determination of sap flow in trees. Plant Cell Environ. 4 pp 391-397.

Cohen, Y., Kelliher, F.M., and Black, T.A. 1985. Determination of sap flow in Douglas-fir tree using the heat pulse technique. Can. for Res. 15 pp 422-428.

Gev, I. 1995. The effect of reforestation in arid sand dune terrain on groundwater recharge and flow system. Ph.D. dissertation, Ben Gurion University of the Negev, Dept. of Geology and Mineralogy, Beer Sheva, Israel (submitted).

Groundwater Resources and Green Construction of the Oil Field of the Taklimakan Desert Heartland

Gao Qianzhao [*]   Wang Run [*]   Sun Liangying [*]

Abstract - According to the survey and drilling experiment along the oil-transporting highway in the desert, there is a certain quantity of available groundwater resources in wake aquifer of fine sediment. Certainly it would provide favorable conditions for vegetable and grasses planting if some key techniques solved. So the groundwater resources on site can be utilized to establish the green parts in the innermost area of the Taklimakan Desert.

Key words: Groundwater resource, Green construction, Salt irrigation, Taklimakan Desert

1. Introduction

It is known that a very large quantity of groundwater resources are reserved in the heartland of the Taklimakan Desert, which is the second largest moving desert in the world, located in the Northwest part of China. Certainly it provides convenient conditions for green construction here. This paper introduces the feeding source, distribution and quality of the groundwater, then provides some experiment of salt irrigation in the heartland, which is the effectual ecological means for stabilising sand and improving the environment of the oil field in the desert.

2. Hydrogeological Conditions and Groundwater Resources in the Desert

2.1 Hydrogeological conditions and feeding source of groundwater

In the Tarim Basin, 13 major rivers have produced a series of alluvial fans throughout the north foot of Kunlun mountains and the south foot of the Tianshan mountain. As a main feature of centripetal river system of inland, a great quantity of river flows toward center part of the basin. Due to the changes of the climate and the influences from human activities, most of the rivers have truncated their end parts so that there is little stream flow outside the oases now, as alternation the part of water feeding into desert groundwater system. So the center part of the basin has been the area of converging, transporting and draining surface water and groundwater, since the lowest part of the basin located in the depression of Lobnor, southeast of the basin. Furthermore, the large basin geological structure and the loose Quaternary sediments not only provide favorable conditions for the storage of deep phreatic water but also give sufficient space for subgroundwater. Moreover, rainstorms and perennial floods as main fresh water sources have fed the groundwater directly and indirectly.

2.2 Groundwater distribution and its quality

The research area referred to this paper is located in the middle part of the desert, within 10 km wide and 230 km long as long as the new oil highway (Fig. 1). Groundwater has been fed by the Tarim River in the northern part of the research area while it by rivers from Kunlun mountains in the southern part. In detail, analysed on flowing direction of groundwater, to the north of Yumulak Daliya (name of a ancient channel), groundwater is mainly restricted by the Tarim River system so the main direction is about from the west to the east; to the south of the mile stone 52 km (K52) of the road, influenced by river system of Kunlun mountains, the main direction of groundwater is NE-15°. Between the two areas two stream

[*] Institute of Desert Research, Chinese Academy of Sciences, Lanzhou, 730000, China (Fax:+86-931-8889950)

systems of groundwater from north and south respectively converge and flow toward east, here with its permeate coefficient is 2-6 m/d.
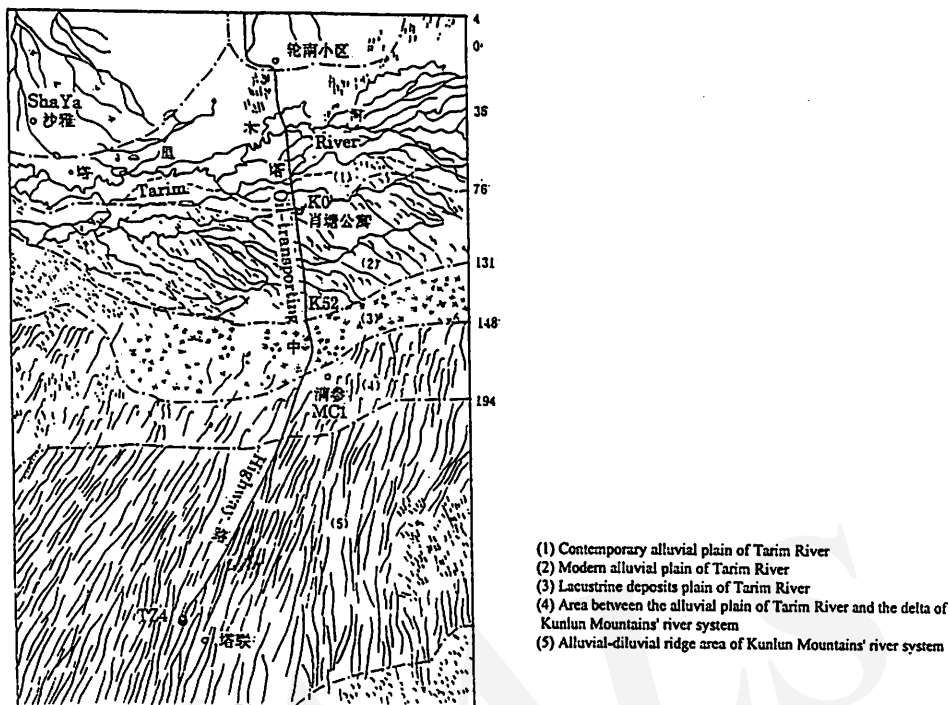

(1) Contemporary alluvial plain of Tarim River
(2) Modern alluvial plain of Tarim River
(3) Lacustrine deposits plain of Tarim River
(4) Area between the alluvial plain of Tarim River and the delta of Kunlun Mountains' river system
(5) Alluvial-diluvial ridge area of Kunlun Mountains' river system

Fig. 1   Sketch Map of Research and Adjoining Area

On the basis of investigation along the oil-transportation road from the Tarim River to TZ4 and drilling experiment, shallow groundwater belongs to silt sand and feeble aquifer. As to its distribution areas, they would be divided into three parts generally according to its feeding sources:

a. Alluvial plain of the Tarim River in the northern part of the research area. Groundwater can be found no more than 5 m under the surface, always 2-3 m. Influenced from perennial floods and fed from the Tarim River, its quality could be fine with its mineralization 1-3 g/l. The available water resources in this part mainly exist in the area of abandoned channels of the Tarim River. Table 1 is the water quality characteristics in one of abandoned channels from drilling experiment.

Table 1. Water quality in an abandoned channel of Tarim River

Drilling Number	Distance from river (m)	Mineralization (g/l)	ph	Fluorine (mg/l)	Chemical Type
C04	0	0.44	7.2	0.68	HCO_3-SO_4-Na-Mg
C05	0	0.54	7.2	1.08	SO_4-HCO_3-Na-Mg
T07	1250	1.74	7.6	3.62	SO_4-HCO_3-Cl-Na
T02	2400	3.73	7.9	1.60	Cl-SO_4-Na
T01	5000	10.19	7.4	0.53	SO_4-Cl-Na-Mg
CK2	50	0.74	7.6	0.79	Cl-HCO_3-SO_4-Na
CK2-G2	106	2.17	7.8		Cl-SO_4-Na

On preliminary estimation the directly available water resources (<1.5g/l) in this area is 1,117,000 m³ which can be extracted in one 1000 m channel in a year. This part of water would be good supply for drinking and other domestic use without any further disposition.

b. River system within Kunlun mountains controlling area in the southern part of the research area. Groundwater in this area often has its mineralization 3-5 g/l covered by high dunes, with little change in the longitudinal section. In the lowland between high dunes groundwater could be found in 2-5 m under the surface. It would provide favorable conditions to utilize this part of water resources for green construction of the oil field.

c. Between the two areas above, groundwater often has its mineralization more than 5 g/l, even 30 g/l found in this area. It is difficult to fully use this part of water at present conditions.

On summary table 2 is overall circumstances of groundwater resources and evaluation on exploitation in the research area.

Table 2. Groundwater resources and exploitation evaluation (10,000 m³)

Area	Water quality	Feeding from sub-runoff	Feeding from precipitation	Amount to depth of layer (mm)	Amount of storage	Suggested extract amount (per km²)
South bank of Tarim River	Sweet water	24.76	0.37	9.3	360	
Alluvial plain and abandoned channels	Sweet water	4.25	8.93	14.5	653.0	150
Kunlun controlling area (lowland between dunes)	Brackish water	87.6	32.48	2.2	1080	160
Between the two areas above	Mineralized and salt water	10.0	1.55	6.5		

3. Green Construction in the Desert Heartland

Some guidable experiment of green ecosystem construction have been done since 1993 at TZ4 and MC1, which are oil field bases in the heartland of the desert. The experiment demonstrates that the salt-resisting species of vegetable, grasses and some other sand-fixing species chosen from the dry zones of the Northern part of China could grow well irrigated with the groundwater of Cl·SO₄-Na·Mg type and 3.4-4.5 g/l of salinity. Although specific techniques and field management are needed, such as taking measures of protection from wind and blown sand harm, irrigating of salt water in high frequency, fertilizing large quantity of manure and hiding the plants from the direct sunlight, dry-hot-wind and high temperature etc., it is successful to establish a small part of green plants among shifting sand dunes. The key techniques solved for green construction in the heartland include how to overcome heavy aeolian sand harm, high Chlorine, Sodium, Magnesium and Boron hazards in groundwater, the poor sandy land with leaking fertilizer and water, environment conditions of extreme drought and high temperature in the air of summer season. 20 species of vegetable and 13 species of grasses with salinity toleration have been selected suitability planting experiment. The results indicate that it is feasible to plant vegetable and green grasses irrigated with local saline groundwater in the greenization construction of oil field in the Taklimakan Desert heartland.

Through the discussion of groundwater resources and green construction experiment above, principles of green construction in the desert could be summarized as following:

a. Constructing saving water and irrigate-with-replenish-water green belts. Small mechanized spray irrigation and trickle irrigation can be through as selected means.

b. Giving priority to salt-resisting shrub on selecting plant species.

c. Dependent upon the scope of oil field base construction, developing small scale green fields, one of feasible measures in the heartland areas.

4. Conclusion

Through the research on the groundwater along the oil-transporting highway and the experiment of the green construction in the heartland area of the Taklimakan Desert, conclusions would be drawn as following:

a. there are two kinds of available groundwater resources in the desert, one is sweet or fresh water which mainly in the alluvial and flooded plain of Tarim River; another kind is brackish water often found in the lowland between sand dunes, which is widespread in the limits of influence of Kunlun mountains;

b. it is feasible to plant vegetable and grasses irrigated with local brackish water on aeolian sandy soils if plant species selected well;

c. techniques and further research on use of salt water, which is reserved over the Taklimakan Desert, need improve and deepen.

References

Chen Guoxiong et al (1995), Preliminary research on vegetable plant in salt irrigation condition in the desert heartland, Journal of Agricultural Ecology, vol. 2, 4,

Chen Moxiang (1965), Groundwater in Xinjiang, Science Press,

Jones K. R. et al (1988), Hydrology in Arid Area, FAO,

Li baoxin and Zhao Yunchang (1964), Groundwater and its formation in the Tarim Basin, Sand Control Research, 6, Science Press,

Gao Qianzhao, Wang Run, Li Xiaoze and Sun Liangying (1994): Preliminary Study on Available Water Resources in the Taklimakan Desert, Chinese Journal of Arid Land Research, vol. 7, 3: 219-224, Allerton Press,

Xia Xuncheng, Li Chongshun and Dong Guangrong et al (1993), Evaluation and Utilization of Water Resources in the Taklimakan Desert, Science Press,

Zhao Songqiao (1985), Physical Geography of Chinese Arid Area, Science Press.

Fate and Transport of Pesticides into Ground Waters

Kenneth K. TANJI*

Abstract - Pesticides applied in desert ecosystems may be of concern, particularly under conditions of elevated temperatures and wind velocities where respectively volatile and aerial drift losses may be substantial, and leaching losses in low organic matter, coarse-textured soils may also be substantial. The fate and transport of applied pesticides are complex requiring some knowledge of their chemical and physical properties, their transformations or degradation, and physical transport processes. Of particular concern is growing problems of contamination of ground waters.

KEYWORDS: Sorption, Volatilization, Persistence, Leaching, Modeling

1. Introduction

Pesticides are formulated in the liquid, gaseous or solid forms and are applied aerially over plant canopies and land surfaces, and incorporated or injected into the soil or into irrigation waters. Applied pesticides can be degraded by chemical reactions and microbial activities in the soil. Pesticides can be immobilized through sorption onto soil organic matter and clay minerals. Pesticides can be lost to the atmosphere through volatilization.

Pesticides that are not degraded, immobilized, detoxified, or removed with the harvested plant are subject to movement away from the point of application. The major loss pathways to the environment are volatilization into the atmosphere and aerial drift, runoff to surface water bodies in dissolved and particulate forms, and leaching into ground water basins (Cheng, 1990). The fate and transport pathways of pesticides applied to ecosystems are complex, requiring some knowledge of their chemical properties, their transformations, and physical transport processes. Transformations and transport are strongly influenced by site-specific conditions and management practices (Porter and Stinman, 1988).

2. Fate and Transport

Chemical-specific properties influence the reactivities of pesticides (EPA, 1986). Pesticides that dissolve readily in water have a tendency to be leached through the soil and vadose zone into ground water basins, and be lost as surface water runoff from rainfall events or irrigation practices. Pesticides with high vapor pressure are easily lost to the atmosphere during application and may be lost from soils through gaseous diffusion. Some highly volatile pesticides may also move downwards into the aquifers. Pesticides may be sorbed to soil particles, mainly organic matter and clays. Strongly sorbed pesticides do not readily leach through the soil profile but may be bound to the sediments discharged through runoff. Pesticides may be degraded or transformed by chemical and biological processes.

* Dept. of Land, Air and Water Resources, Hydrologic Science Program, Univ. of California, Davis, California 95616 (Fax: +1- 916-752-5262)

Chemical degradation occurs through such reactions as photolysis, hydrolysis, and oxidation and reduction. Biological degradation may also occur as soil microbes consume or breakdown pesticides. Oxidation and reduction may be mediated by microbial activities.

Once a pesticide enters the soil, its fate is largely dependent on sorption and persistence (Rao and Hornsby, 1989). Sorption is commonly evaluated by use of a sorption (partition) coefficient (Koc) based on the organic carbon content of soils. Persistence is commonly evaluated in terms of half-life and is dependent on degradation and transformation mechanisms. Pesticides with low Koc are likely to leach from soils. Pesticides with long half-lives could be persistent. And pesticides with high water solubility is likely to contaminate ground waters.

Soil properties have significant influences on the fate and transport of pesticides. The infiltration rate and soil hydraulic conductivity of coarse-textured soils are usually greater than those of finer-textured soils. A chemical that readily infiltrates into the soil is less likely to be lost in surface runoff but is more likely to be leached. The travel time of soil water and associated dissolved pesticides is shorter in coarse-textured soils than in finer ones. Moreover, the sorptive capacity of coarser textured soils are less than finer ones and the applied pesticides are more vulnerable to leaching.

Soil structure is another property of importance. A soil with weak structure is more likely to be erodable and have lower infiltration rates, and hence, sorbed pesticides are more likely to be discharged through surface runoff. The presence of soil macropores and cracks may result in preferential flow and earlier pesticide arrival to the water table. A shallow depth to the ground water table offers less opportunities for pesticide sorption and degradation. Hydrogeologic conditions in the subsurface may dictate the direction and rate of chemical movement. The presence of water-impermeable layers may constrain the vertical movement of chemicals and contribute to lateral flow. On the other hand, the presence of sands and gravel may greatly accelerate the vertical and horizontal flow of contaminants. Karst and fractured geologic formations generally transmit chemicals rapidly.

Climate and weather conditions other than rainfall may also influence the fate of pesticides. Warmer temperatures tend to accelerate physical, chemical and biological processes such as volatility, water solubility and microbial degradation, respectively. High winds and high evaporative conditions may accelerate volatilization and other processes that contribute to gaseous losses of pesticides

Despite the vast knowledge base on the reactivity and transport of pesticides, a complete mass balance on the fate of applied chemical is nearly nonexistent because of technical difficulties and high cost associated in developing mass balance (NRC, 1993). Moreover, pesticides have widely ranging properties and behavior that defy generalizations. Some researchers have estimated that only 1 to 2% of insecticides applied to foliage is absorbed by the target pest.

3. Screening Models

A number of pesticide screening approaches have been used to assess the behavior of pesticides and their potential to contaminate ground waters. One of the more widely used screening models is EPA's (1986). Table 1 presents the threshold values for several properties and DBCP is compared to them (Tanji, 1991). DBCP (Dibromochloropropane) was a widely used nematicide for numerous vegetable, field, orchard, and vine crops from the mid 1950s to 1979 when it was banned from use in the USA due to potential carcinogenity and male sterility. DBCP is resistent to chemical and microbial degradation, not strongly sorbed to soils, moderately soluble and not highly volatile. A conclusion may be reached that DBCP is a persistent chemical likely to be leached into ground water basins. And indeed, this chemical is one of the most common pesticide residues found in contaminated ground waters in California, Florida and Hawaii.

Table 1. DBCP vs. EPA threshold values for potential ground water contamination

Properties	Threshold Values	DBCP
Water solubility (mg/L)	> 30	700 - 1,230
Henry's Law Constant (atm m^3/mol)	<100	212 - 380
Koc Sorption (L/Kg)	<300-500	305 - 355
Hydrolysis Half-Life (weeks)	>25	2,000 - 7,600
Photolysis Half-Life (weeks)	>1	0.002 - 0.3
Overall Field Half-Life (weeks)	>3	1.7 - 2,000+

4. Simulation Models

A number of computer simulation models are used as tools to evaluate more fully the fate and transport of pesticides, including spray, runoff and leaching models (Cheng, 1990). The process-based simulation models for pesticide reactivity and transport are receiving much attention in the USA (NRC, 1993). The field scale models include EPIC (erosion/productivity impact calculator), GLEAMS (groundwater loading effects of agricultural management systems), PRZM (pesticide root zone model), and LEACHM-P (leaching estimation and chemistry model-pesticides). A number of investigators point out difficulties in predicting chemical ground water contamination even with state-of-the-art simulation models. The convection-dispersion models appear unable to predict pesticide transport in the vadose zone. The reasons contributing to this dilemma include spatial variability in soil hydraulic

properties usually encountered in field soils, the potential nonequilibrium sorption in the field, the depth dependency of biodegradation, and preferential flow through macropores.

Pennell et al (1990) compared the performances of five vadose zone models for simulating the behavior of aldicarb and bromide in a given field. The models tested were CMLS (chemical movement in layered soils model), MOUSE (method of saturated zone solute estimation model), PRZM, GLEAMS, and LEACHM-P. Two models, GLEAMS and MOUSE, under estimated bromide and aldicarb dissipation. The other three models proved satisfactory in predicting both the depth of the solute's center of mass and the extent of pesticide degradation. None of the models, however, accurately predicted the pesticide concentrations measured throughout the soil profile. In addition to deficiencies in the model, the investigators pointed out the potentially large field sampling error due to spatial variabilities. Most recently, a concerted effort is being made on understanding and assessing the uncertainty in transport as well as reactivity of chemicals with conditional stochastic methods (e.g., Kabala and Sposito, 1994).

5. Conclusions

There is considerable knowledge base about the physical and chemical properties of pesticides, their chemical and biological degradation and persistence, their tendency to be sorbed by soils, and their movement in the dissolved and gaseous states. In contrast, our abilities to predict the behavior and transport under field conditions appear to be quite weak. Part of this weakness may be attributed to spatial heterogeneity of both soil hydraulic properties and reactivity of chemicals. This uncertainty is elevated in arid climates in which temperatures and wind velocities are high, and the vadose zone and ground water systems may not be adequately characterized. Nevertheless, it seems that the existing knowledge base from research and practical experiences is not being fully disseminated or utilized to protect the environment.

6. References

Cheng, H.H., ed. 1990. Pesticides in the Soil Environment, Soil Science Society of America Book Series No.2.

Environmental Protection Agency. 1986. Pesticides in Groundwater Document.

Kabala, Z.J., and Sposito, G. 1994. Water Resources Research 30(3):759-768

National Research Council. 1993. Soil and Water Quality, National Academy Press

Pennell, K.D., Hornsby, A.G., Jessup, R.E., and Rao, P.S.C. 1990. Water Resources Research 26:2679-2693.

Porter, K.S., and Stinman, M.W. 1988. Protecting Groundwater, Cornell Univ. and Univ. of California, Davis.

Rao, P.S.C., and Hornsby, A.G. 1989. Fact Sheet, Univ. of Florida .

Tanji, K.K. 1991. Seminar, Univ. of California, Davis.

Contents

Original Articles

Poster Papers without review

Contents: <u>Poster Papers without review</u> *(Continued)*

<u>Posters & Exhibitions without Paper</u>

<u>Videos without Paper</u>